UNIVERSIDADE DE LISBOA

FACULDADE DE CIÊNCIAS

DEPARTAMENTO DE GEOLOGIA

Non-coaxial progressive deformation vs. overlapping of different deformation phases: detailed geological-structural survey in the key area of Perais (southern edge of the CIZ)

Maria Inês Viegas Roque da Silva

Mestrado em Geologia
Especialização em Geodinâmica e Recursos Geológicos

Versão Provisória

Dissertação orientada por:
Filipe Rosas
Ícaro Dias da Silva

2025

Acknowledgements

I am grateful for the support of several generous individuals who made this work possible.

First and foremost, I would like to express my gratitude to my parents, João and Cristina, for their unwavering belief in me, their full support, and their investment in my education.

I would like to extend my thanks to my supervisors, Professor Filipe Rosas and researcher Ícaro Dias Da Silva, for their guidance and support throughout the process.

Special thanks to researcher Ícaro Dias da Silva for his exceptional support, without which this work would not have been possible.

I am grateful to Professor Filipe Rosas for imparting geological knowledge and contributing to the development of my critical thinking.

I would also like to thank researcher Jaime Almeida, who provided continuous support throughout the process despite not being my supervisor.

Gratefull for the priceless help of the lab technician Sofia Rodrigues.

Lastly my heartfelt thanks to my colleagues and best friends, Joana Tavares Perfeito Amaral, Maria Inês Venda Duarte da Silva, and Sara Recto Moutinho, for their unwavering support and encouragement.

I am eternally grateful to all of you for making this work possible. Thank you.

Abstract

The main objective of this study was to identify and characterize the deformation events in the study area in Perais. The geological study of the Perais region, located 16 km southeast of Castelo Branco, examines the deformation events that have occurred over time. The area is in the Central Iberian Zone and is part of the Schist Graywacke Complex. Three orogenies affected the region: the Cadomian, the Variscan, and the Alpine, two of them successfully identified in the studied Perais area.

The Cadomian Orogeny generated regional unconformities, while the Variscan Orogeny, with four compressive and two extensive phases, produced folds, faults, and shears. The Alpine Orogeny resulted in brittle deformation, uplift, erosion and crustal shortening due to the convergence between the African and Eurasian tectonic plates.

Detailed structural geology mapping led to the recognition of three ductile deformation events affecting the detrital Malpica do Tejo Formation (pelites, greywackes and conglomerates) and different generations of quartz veins. The micro-tectonic study carried out by the careful observation of a number of oriented thin sections revealed different stages of ductile deformation, with evidence of heterogeneous deformation.

This study concludes that the deformation observed in the Perais area is possibly related to the Variscan phases of deformation, specifically to the regional stages D_1-M_1 (ductile folding), D_2-M_2 (crenulation and shear deformation) and D_3-M_3 (upright heterogeneous folding), since there is not enough evidence to associate these with the Cadomian Orogeny by lacking clear cross-cutting or overprint structural relationships.

Keywords: Structural geology, microtectonics, ductile deformation, Variscan orogeny

Resumo

A problemática da deformação ao longo de zonas de cisalhamento associadas ao regime de cisalhamento simples, tem sido objeto de estudo, quer em zonas afetadas por alto grau como em baixo grau metamórfico.

A área em estudo, localizada nas imediações do parque de merendas de Perais, localiza-se a 16 km a sudeste de Castelo Branco, na margem direita do Rio Tejo. Inserida na folha 28-B (Nisa) do Mapa Geológico de Portugal a escala 1:50000 e na folha 6 do Mapa Geológico de Portugal a escala 1:200000, apresenta uma complexidade de estruturas nunca estudadas até ao momento e que não estão presentes em estudos acima referenciados.

Geologicamente, os afloramentos estudados encontram-se na Zona Centro Ibérica (ZCI), mais concretamente na Formação Malpica do Tejo pertencente ao Grupo das Beiras do Complexo Xisto-Grauváquico. As principais litologias correspondem a uma sequência turbidítica siliciclástica formada em ambiente do tipo *back-arc* da orogenia Cadomiana de idade Ediacárica compreendendo rochas metapelíticas, metasiltíticas e metagrauváquicas deformadas em regime dúctil na fácies dos Xistos Verdes.

A Formação Malpica do Tejo (de idade Ediacarica) é a unidade mais baixa estratigraficamente da ZCI no setor estudado e apresenta evidencias excecionais de deformação dúctil que até agora nunca tinham sido estudadas. O seu tramo inferior, representado nos afloramentos do parque de merendas de Perais, é composto maioritariamente por bancadas de arenitos impuros e grauvaques de potencia métrica, cuja estratificação foi transposta por um *fábric* planar de origem tectónica.

Pode ser assumido, dada a idade e posição estratigráfica desta formação, que a sua sequência foi afetada por eventos de deformação associados a três orogenias, como a Cadomiana (Neoproterozoico superior), a Varisca (Paleozoico superior) e a Orogenia Alpina (Meso-cenozoico).

A orogenia Cadomiana, que ocorreu na margem do continente Gondwana, está associada à formação de um arco magmático relacionado com uma zona de subducção. Esta orogenia gerou um conjunto de superfícies de inconformidade estratigráfica, identificadas num setor próximo a este em Espanha, durante o Ediacárico (discordância Alcudiana) e na transição para o Paleozoico inferior (discordância basal do Câmbrico) estando neste último caso, relacionado com a passagem tectónica de uma margem ativa para uma margem passiva.

A orogenia Varisca afetou a região através de quatro fases de deformação regionais compressivas e duas fases extensivas. A primeira fase compressiva gerou dobras subverticais de direção WNW-ESE, com vergência para NNE associado a movimentos transpressivos esquerdos, enquanto a segunda fase compressiva é apenas observada nas regiões limítrofes aos complexos alóctones da Zona Galiza-Trás-os-Montes, associada à instalação ao longo do orógeno de um prisma de acreção Varisco desenraizado. A terceira fase de deformação Varisca corresponde à primeira fase extensional associada ao colapso gravítico sinorogénico do orogeno que favoreceu o adelgaçamento crustal e a formação de zonas de cisalhamento sub-horizontais num regime termo-barométrico de alta temperatura e baixa pressão regional. Posteriormente, o terceiro evento compressivo foi responsável pelo dobramento desarmónico sub-vertical e pelo aparecimento de zonas de cisalhamento conjugadas que afetam e verticalizam as estruturas anteriores. Finalmente, as duas últimas fases de deformação estão associadas ao levantamento tectónico associado à compressão continental fini-orogénica que originaram um conjunto de zonas de cisalhamento frágeis sub-verticais e sub-horizontais contemporâneas da instalação de granitos tardi- a post-tectónicos na ZCI.

A orogenia Alpina, que se encontra ativa desde o final do Mesozoico, caracteriza-se pela (re)ativação dos sistemas de falha variscos de forma frágil, induzindo o levantamento tectónico

da Península Ibérica síncrono da sua rotação sinistrogira, favorecendo a erosão e criando a topografia atual, devido a aproximação da placa Euroasiática com a placa Africana.

O objetivo principal deste estudo é caracterizar a deformação dúctil associada ao padrão de dobramento dos veios de quartzo nos afloramentos de Perais, definindo as geometrias condições de deformação cinemática das estruturas identificadas. Para tal, realizaram-se trabalhos de campo consistindo no levantamento de dois cortes geológicos e na realização de uma cartografia geológica-estrutural de detalhe numa zona chave da margem direita do Rio Tejo, procedendo-se à recolha de medições estruturais e de amostras orientadas para a realização de lâminas delgadas, compilando informação fotográfica. O trabalho de campo foi complementado pela observação e caracterização da deformação à microescala, aplicando-se os procedimentos clássicos do estudo da microtectónica, de forma a poder identificar as diferentes fases de deformação, as geometrias de deformação e a cinemática associada.

Foram identificados veios de quartzo de diferentes gerações, dispostos em diversas orientações, sendo possível identificar 3 famílias distintas. A primeira família, mais precoce e mais abundante com uma direção NNW-SSE apresenta evidencias de defomação dúctil. A segunda e a terceira família, de aspeto mais retilíneo, apresentam direções NE-SW a N-S.

Os veios de quartzo pertencentes à família mais precoce, de uma forma geral apresentam-se dobrados, boudinados, definindo dobras boudinadas ou boudins encavalitados. A caracterização grométrica deste padrão estrutural complexo foi realizada de forma a obter uma visão tridimensional. Desta forma, foram realizadas lâminas delgadas em duas direções, uma paralela à lineação de estiramento/transporte tectónico e outra perpendicular, correspondendo, a grosso modo, às vistas em corte e planta dos afloramentos estudados.

A mineralogia identificada em lâmina delgada corresponde a uma associação de biotite (localmente substituída por clorite), quartzo (relíquia e em veios), plagioclase (detrítica), óxidos e sulfuretos, que caracterizam o metamorfismo na fácies dos Xistos Verdes, com pico térmico na zona da biotite, contemporânea da deformação em regime de cisalhamento simples associado à formação e deformação dos veios de quartzo.

Para além da identificação mineralógica no estudo das laminas delgadas; a identificação de estruturas que os minerais formam permitem retroceder os eventos deformativos á microescala e posteriormente reconstruir uma sequência de eventos deformativos que será palicada á macro escala.

Nas secções paralelas à lineação de estiramento (secções A) foram identificadas bandas de cisalhamento C e C' com uma foliação principal associada (S_n), com cinemática de topo para SSE (su-sudeste) e ESE (és-sudeste), que influenciou a boudinagem a formação de dobras intra-foliares dos veios de quartzo e provocou a completa transposição do fabric. Nas secções B, perpendiculares às anteriores, observou-se complementarmente que os fábrics anteriormente descritos se encontravam dobrados (com S_{n+1} de plano axial) e crenulados por um evento posterior, correspondente à verticalização da estrutura associada a S_n. Também foi possível identificar nos "microlithons" da foliação principal S_n uma foliação tectónica anterior (Sn-1), não identificável em afloramento.

Esta sequência de eventos de deformação poderá corresponder em termos regionais, às três fases de deformação Variscas. Deste modo, a foliação local S_n pode corresponder à foliação Varisca S_2, associada ao evento extensional D_2-M_2, com vestígios de uma deformação mais antiga (D_1-M_1). A deformação também envolveu uma compressão tardia (D_3), com dobramentos e a formação de uma clivagem do plano axial S_3. Não foram identificadas evidências suficientes para confirmar a presença de deformação Cadomiana.

Conclui-se que o estudo da zona de merendas de Perais revelou um complexo processo de deformação ligado ao ciclo orogénico Varisco, afectando o Complexo Ediacarano de Xistos e

Grauvaques da Zona Centro-Ibérica. A deformação incluiu o dobramento de veios de quartzo, a transposição de camadas e o desenvolvimento de múltiplas gerações de "fabrics" observadas ao microscópio petrográfico. No processo foi identificado três fases principais de deformação: dobramento e foliação inicial na zona de clorite, seguido de cisalhamento simples dúctil e dobramento complexo de veios de quartzo na zona de biotite, e dobramento tardio que conduziu a uma deformação frágil com geração de falhas e "kink-bands". Estas fases alinham-se com o ciclo tectono-metamórfico Varisco (D1, D2, D3), não havendo evidência de deformação cadomiana na região.

Palavras-Chave: Geologia Estrutural, microtéctonica, deformação dúctil, Orogeno Varisco

Index

Figure index

1. Introduction

The study of local or regional structures allows the identification of deformation events that occurred in an area or in a rock specimen. It reveals the tectono-metamorphic events and the thermal-barometric conditions to which a specific section of the lithosphere has been subjected. Detailed study of deformation is therefore important to understand these processes at all scales.

Non-coaxial deformation, a style of progressive deformation that occurs over a defined space interval, happens when stress manifests itself in different ways at two points with the same driver. Its main characteristics is its strong rotational component, which leads to different angular relationships with the three principal directions of stress along time, producing different overlapping tectonic fabrics and generating different responses to local and bulk strain.

This type of deformation gives rise to heterogeneously distributed structures that can be misled with different deformation events.

Considering this, the main objective of this study is to gain a better understanding of the phases and style of deformation observed in a critical exposure of the Beiras Group of the Schist and Greywacke Complex at the southern edge of the Central Iberian Zone (CIZ) affected by a low-metamorphic grade, quartz vein-rich shear zone. To achieve this, it was undertaken a detailed examination in two road sections and a riverbed exposure in the Tejo River right margin near Perais village, in Castelo Branco, Portugal.

This area exhibits a complex pattern of geological structures that affect the Ediacaran detrital rocks of the Beiras Group in the CIZ. This pattern is further emphasized by the presence of multiple generations of quartz veins and veinlets that have been installed in the pelitic-greywacke metasediments. The observed succession of events may be related to one or more phases of deformation and/or to coaxial or non-coaxial deformation regimes.

Reconciling studies of the deformation at meso- and microscale and the structural geological survey in the cross sections and riverbed exposures in Perais, the type of deformation that has affected these metapelite rocks will be revealed, whether it was produced throughout different phases/stages of stepped coaxial deformation regimes or from continuous non-coaxial deformation.

2. Geological Setting

The Perais village picnic area (Fig. 2.1) is located 16 Km SE of Castelo Branco, in the right margin of the Tejo River. It is inserted in the northernmost boundaries of the Sheet 28-B (Nisa) of the 1:50 000 scale Geological Map of Portugal, (Ribeiro et al., 1964) and of the sheet 6 of the 1:200 000 scale Geological Map of Portugal (Ferreira & Piçarra, 2020).

Geologically, this area (Fig. 2.1C) is in the southern part of the Central Iberian Zone (CIZ), one of the Iberian Massif tectono-stratigraphic domains of the Variscan Belt (e.g. Julivert et al., 1972; Dias da Silva et al., 2021 - Fig. 2.1A, B). The Variscan Belt was formed by the continental collision between Gondwana and Laurussia that came after the closure of the Rheic Ocean in the late Paleozoic (e.g. Martínez Catalán et al., 2009; Pereira et al., 2009; Díez Fernández et al., 2016).

1
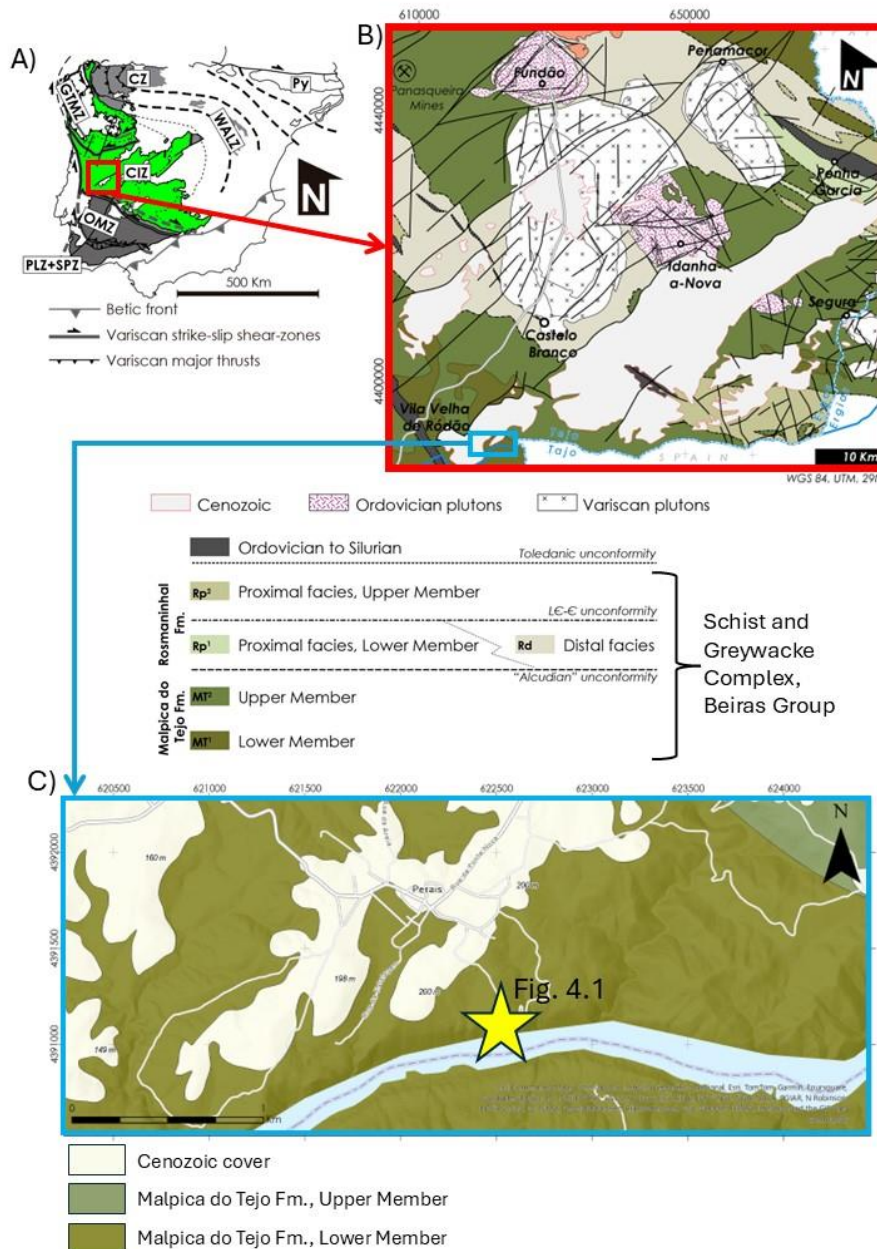
Figure 2.1 – Location of the study area. A) Sketch map of the Iberian Massif: OMZ, Ossa–Morena Zone; CIZ, Central Iberian Zone; CZ, Cantabrian Zone; GTMZ, Galicia–Trás-os-Montes Zone; PLZ, Pulo do Lobo Zone; SPZ, South Portuguese Zone; WALZ, West Asturian Leonese Zone (simplified from Martínez Catalán 2011); B) Simplified geological map of the southern part of the Central Iberian Zone. Adapted from the 1:200.000 geological map of Portugal (sheet 4) (Meireles 2020) and from Ferreira da Silva (2013). Taken from Dias da Silva et al. (2023); C) Detail of the studied area with the Perais picnic area marked with a yellow star. Adapted from the 1:50000 geological map of Portugal (Folha 28-B - Nisa) (Ribeiro et al. 1964).

2.1   Stratigraphy

The CIZ is characterized by a stratigraphic sequence that includes Ediacaran to late Carboniferous siliciclastic formations, deposited during three major geodynamic cycles: the Ediacaran-lower Cambrian Cadomian orogeny (e.g. Pereira et al., 2012; Chichorro et al., 2023), the Lower Paleozoic opening of seaways and oceans in the northern Gondwana margin (e.g. Garfunkel, 2015), and the Variscan orogeny related to the continental collision that produced Pangaea in the Late Paleozoic (Martinez et al., 2014). Wide areas of the CIZ in Portugal, present large plutonic

2

complexes, ranging from the Cambrian-Ordovician (e.g. Pereira et al., 2022) to the early Permian (Rodriguez et al., 2004), which mark important stages of these geodynamic events and can be used to date the maximum and minimum ages of the deformation regionally and metamorphic events in this region.

Most of the exposed stratigraphic record in the southern-central section of the CIZ is dominated by Ediacaran-lower Cambrian flysch mega-sequences, including siliciclastic (pelitic, greywacke and conglomeratic facies) and minor arc-type volcanic rocks (Sousa, 1984; Rodríguez Alonso et al., 2004; Ferreira da Silva, 2013). These were deposited in a back arc basin of the Cadomian orogen thus marking evidence of high temperature metamorphism in an active magmatic arc and its by-products (e.g. Pereira, et al, 2012). This sequence is included in the Schist and Greywacke Complex (SGC), which can be divided into Beiras and Douro Groups (Sousa, 1984; Pereira,1987; Sousa and Sequeira, 1987, 1989; Ferreira da Silva, 2013).

The Schist and Greywacke Complex in the studied sector is composed of the Ediacaran-lower Cambrian Beiras Group. It presents, from bottom to top, the Malpica do Tejo Formation (Lower and Upper Members; Ferreira da Silva, 2013) and the Rosmaninhal Formation (Lower, Distal and Upper Members; Ferreira da Silva, 2013). The Lower Member of the Malpica do Tejo Fm. corresponds to the Lameira da Ordem-Palhota unit (Romão et al, 2000), and the Upper Member corresponds to the S.Pedro do Esteval unit (, 2000) in the Geological Map of Portugal.

The sequences of the Malpica do Tejo Formation show different polarities depending on the area under observation. In the areas contiguous to the Tejo River, between Mação-Vila de Rei and Castelo Branco-Monfortinho-Rosmaninhal it shows a negative polarity and in the northern regions, from the Bouçã and Cabril reservoirs, the Moradal, Guardunha and Penha Garcia to Arouca and the Estrela and Malcata mountains a positive stratigraphic sequence (Ferreira da Silva, 2013). The study area presents negative sequences, with the lower member made of millimeter to centimeter-thick sequences of metapelites, metasiltites, metagreywackes and conglomerate beds; the progression to the upper limb is marked by a gradual increase in thickness and frequency of meta-greywacke beds (Ferreira da Silva, 2013).

2.2   Deformation

2.2.1   *Cadomiam orogeny*

The Cadomian orogeny occurred during the late Neoproterozoic – earliest Cambrian (650-550 Ma) (e.g. Linnemann, et al., 2008; Pereira et al., 2012; Chichorro et al., 2023). This orogeny is recorded along the northern margin of the Gondwana continent, where an accretionary orogen and back arc basins were generated (e.g. Fuenlabrada et al., 2020). This orogeny is marked by two regional unconformities related to the orogenic overprint of the sedimentary sequences (Alcudian unconformity) (e.g. Talavera et al. 2015) with folding and bedding transposition (Valladares et al., 2000) followed by a period of tectonic inversion from a compressional to an extensional regime that dominated the opening of the Rheic Ocean and subsidiary seas in the lower Paleozoic as result of the widening of the Cadomian backarc in north Gondwana (e.g. Murphy et al., 2006), which lasted from the early Cambrian to the Early Devonian (e.g. Orejana et al., 2015; Gutierrez Marco et al., 2019; Sánchez García et al., 2019). This late Cadomian inversion is interpreted in terms of the birth of an intracratonic rift, located to the south-west of the Ossa-Morena Zone (OMZ), present coordinates.

2.2.2   *Variscan Orogeny*

The second orogenic cycle in this region is related to the continental collision that followed the

consumption of the Rheic Ocean which produced the Variscan Orogen, which occurred between the Upper Devonian to the uppermost Carboniferous. According to Martínez Catalán et al. (2014) and Dias da Silva et al. (2021), the tectonic-metamorphic evolution of the Variscan mountain chain, the Central Iberian Zone underwent four compressional (C) and two extensional phases (E) that are synchronous with three regional metamorphic stages: M_1, of Barrovian type and locally high pressure metamorphism, M_2 Buchan type high temperature-low pressure metamorphism and M_3 retrograde metamorphism (Dias da Silva et al., 2021) (Fig. 2.2). In this way, these compressional and extensional stages can be grouped in 3 regional deformation-metamorphic events, named as D_1-M_1 (including C_1 and C_2 structures), D_2-M_2 (including the E_1 stage) and D_3-M_3 (grouping C_3, C_4 and E_2 stages).

2.2.2.1   1st Compressional phase (C_1-M_1)

The first Variscan deformation phase, C_1, is responsible by the production of tight and almost isoclinal folding and the generation of transcurrent shear zones, which were created under regional greenschist metamorphic environment during the Upper Devonian (370-360 Ma; Dallmeyer et al., 1997). High pressure metamorphism is only observed in the NW Iberia Upper and Lower Allochthonous Units of the Galicia-Trás-os-Montes Zone (GTMZ), in the southern Ossa Morena Zone (OMZ) and along the boundary of the OMZ with the CIZ related to subduction and obduction of continental crust in the Variscan accretionary wedge (e.g. Moita et al., 2005; Martínez Catalán et al., 2007; Arenas et al., 2017, 2021). In the CIZ folds produced an axial planar cleavage S_1, with vergence to different directions (depending on which zone is being observed), with long normal limbs and short reversed limbs (e.g. Díez Balda et al., 1990; Dias et al., 2013). The C_1 folding in the studied sector, is represented by sub-vertical WNW-ESE and NNE verging folds formed under the influence of a left transpessive shear regime. This phase is responsible for the main crustal thickening event of the Variscan orogeny.

2.2.2.2   2nd Compressional phase (C_2-M_1)

The second compressional phase occurs only at NW Iberia as the result of the thin-skinned imbrication of the GTMZ allochthonous and parautochthonous units onto the CIZ in the lower Carboniferous (350-340 Ma) (Dallmeyer et al., 1997). The deformation was induced by the imbrication of the Upper Parautochthon (UP) onto the Lower Parautochthon (LP) along a major structure known as the Main Trás-os-Montes Thrust (MTMT) and by the stacking of the LP onto the CIZ using the Basal Lower Parautochthon Detachment (Dias da Silva et al., 2021). This stage was responsible by the folding of the C_1 stage folds producing the major drag fold defined as Central Iberian Arc or Curve, and it was locally responsible by the baric peak in the CIZ (Martinez Catalán, 2012; Pastor Galán et al., 2019; Dias da Silva et al., 2021).

2.2.2.3   1st Extensional phase (E_1-M_2)

The first extensional phase is related to the synorogenic isostatic rebound and crustal thinning that followed the initial C_1+C_2 crustal thickening, being active from the Visean to the Baskirian age (340-320 Ma) (Escuder Viruete et al, 1994, 1998; López Moro et al., 2018). It is characterized by an increasing thermal readjustment of the crust by fast rising of the middle/lower crust domains towards the surface, related to the release of the tectonic overload and isostatic balance; this resulted in the rapid exhumation and in a regional partial melt of the crust and upper mantle, favoring the formation of gneiss dome structures and their migmatite cores. These major structures are structurally controlled by gently dipping to sub-horizontal extensional shear zones with parallel S_{E1} tectonic banded, that mimic the M_2 isogrades of the Buchan type (HT-LP)

metamorphism, promoting the genesis of oval-shaped basins and gneiss domes which gradually invaded upper crust domains, locally overprinting the previous structures and metamorphism (e.g. Dias da Silva et al., 2021).

2.2.2.4   3rd Compressive phase, C_3-M_3 (uplift and retrogression)

This stage marks the regional retrograde deformation caused by uplift during Variscan crustal thickening. In the initial stages (~318-310Ma) it developed the regional upright folding with WNW-ESE to NW-SE axis and steep cleavage of the previous structures (e.g. Pastor Galán et al. 2019). Later (~310-300 Ma), the C_3 phase has produced sub-vertical conjugated transcurrent shear zones that specially affected the gneiss dome cores and the Variscan granitic plutons (e.g. Gutiérrez Alonso et al., 2015; Díez Fernández and Pereira, 2017), which allowed the accommodation of stress during the formation of the Iberian-Armorican Arc that marked the regional oroclinal bending of the previous structures in the Carboniferous-Permian transition (e.g. Weil et al., 2010). In the areas where C_2 and E_1 structures are absent, third compressional phase is easily mistaken with the first compressive event because they are coaxial and present identical geometries (Pastor Galán et al. 2019).

2.2.2.5   2nd Extensive (E_2) and 4th Compressive phase (C_4) – Post Variscan orogenic collapse and final uplift

These deformation phases affect all the previous ones and are responsible for extensional faults and sub horizontal folding and kink-band structures related to gravitational collapse. The C_4 compressional phase was responsible for the formation of brittle NNE-SSW and NNW-SSE faults and associated sub-vertical kink-bands (e.g. Dias da Silva et al. 2021).

5
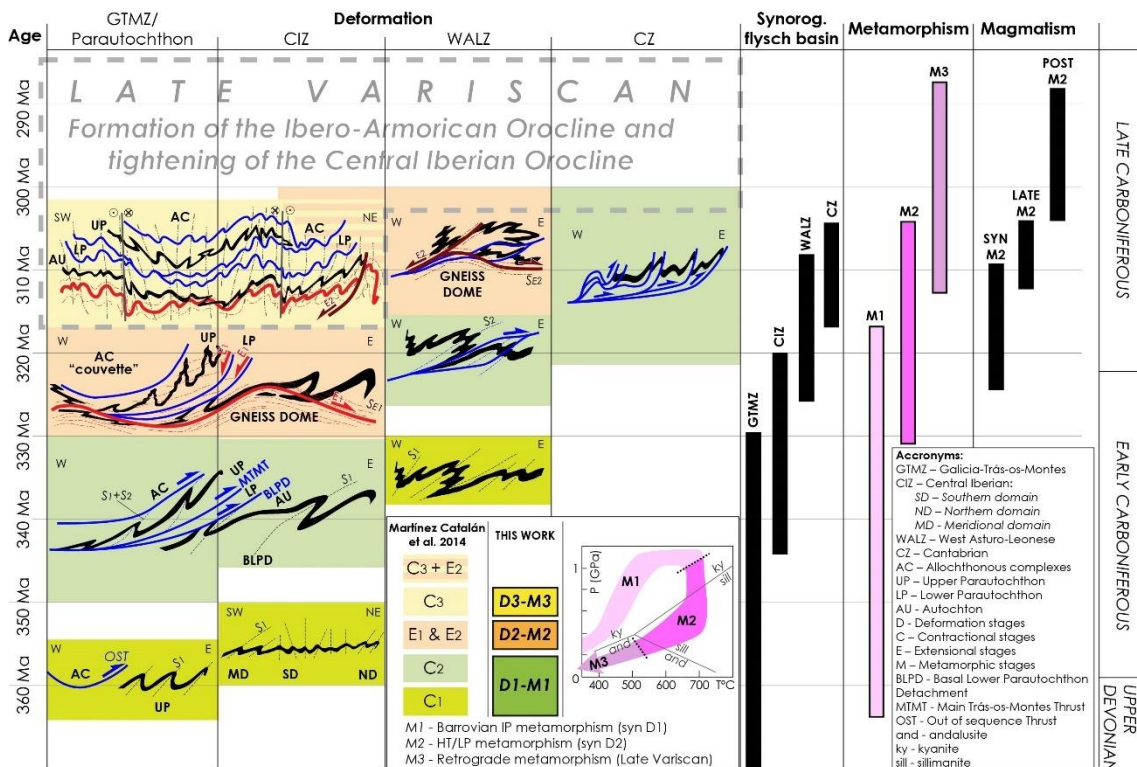
Figure 2.2 – Deformation and metamorphism stages in the Iberian Massif. Taken from Dias da Silva et al. (2021).

2.2.2. *Alpine Orogeny*

This region suffered deformation during the Alpine Orogeny, which has been active since the Mesozoic. In the study area the deformation related to this orogenic period can be subdivided into two stages.

The first stage, between Triassic and latest Cretaceous (Ellouz et. al., 2003), corresponds to tectonic quiescence and erosion. This erosive event is responsible for the disappearance of the Variscan topography and the tectonic is contemporaneous with extensional orthogonal rifting with transtension movement. The second stage reflects the results from the approximation of the African and Eurasian plates, between the Late Cretaceous and the Oligocene with N-S direction with a rotation afterward to NW-SE in Late Miocene. This approximation has conducted to a crustal shortening that was later accommodated in an alternation of roughly E-W basement uplifts and basins as well as in a NNE-SSW oblique strike-slip fault corridors at the western border of the Iberian Massif.

3. Objectives

The primary goal of this study is to find the original bedding and to understand the deformation that led to the deformation of quartz veins. It is important to determine the number of deformation events, types and metamorphic conditions in the of the Malpica do Tejo Formation outcrops of the Perais picnic area. It was necessary to identify folding patterns, boudinage evidence and related tectonic fabrics that affect original bedding and the quartz veins and veinlets in this natural laboratory. Field geology combined with microtectonics studies of selected samples is applied, as has it has been proven to be a very effective method for observing and differentiating multiple deformation events, as it enables the identification of in-situ evidence and the detailed analysis of fabrics from the outcrop scale to thin section.

4. Methods

As the focus of this study is to identify the different deformation phases in the Perais slate and greywacke exposures, there is no better way to study the deformation than structural geology field work, as a starting point. This chapter aims to present the methodologies used, as well as the procedures, in the various stages of the work, which are required for answering the scientific questions approached in this thesis: how many deformation and metamorphic stages are affecting the rocks in the studied outcrops and what tectonic regimes were acting to produce the deformation patterns shown by the quartz veins and veinlets within the slates and greywackes in the studied outcrops. All the sample preparation procedures took place in the laboratories of FCUL's Geology Department.

4.1   Fieldwork

The methodology of field geology is to collect information using various methods based on the nature of the study object whether for geophysics, geochemistry, cartography, hydrogeology, among others. In this case, fieldwork was applied for structural geology and geological mapping, using appropriate methodology to carry out geological surveys and collect carefully selected samples.

Fieldwork was divided into four parts: 1) Identification, selection and structural sketching of two

geological cross-sections; 2) detailed mapping of geological structures in the Tejo riverbed exposures; 3) collecting oriented samples for microtectonics studies and 4) photo report for cabinet interpretation of meso- and micro-structures. Structural information was compiled to produce a database with systematic measurements of tectonic fabrics for stereographic projection and structural analysis of foliations and lineaments.

4.1.1 *Geological cross-sections*

The study of geological cross-sections is one of the most used methodologies in geology. It has proven of great value as it can be used to make regional generalizations in areas where outcrops are scarce and gives the geologist an opportunity to observe and collect data in a systematic and reliable way in the field. The importance of studying outcrops in road cuts to produce detailed cross-sections, is the availability of the lithologic information that the geologist can identify, including a three-dimensional view on the structures, to reveal geometrically accurate information that allows more concise (kinematical and when possible dynamic) interpretations. Structural data can be retrieved using a geologist compass or a mobile application to gather planar (e.g. bedding, foliations, fault planes) and linear (e.g. stretching and intersection lineations, fault striae, fold axis, etc.) data using a simple nomenclature (e.g. dip/dip azimuth, right hand rule) that can be stereographically projected to be used as a basis for structural interpretations and/or statistical analysis of these collected structural data.

In the study area it was possible to observe the intersection of geological structures with the surface in two road sections that are sub perpendicular to the main direction of most observed structures, which allowed a 3D view of the geological structures affecting the Malpica do Tejo Formation in this region (Fig. 4.1). The main structures measured in these road sections are bedding (S_0), folds (axial planes, fold axis and limbs), faults (fault plane attitudes and striae), main foliation (S_n, transposing the bedding) and its late folding evidence. In these same surfaces of exposure was also possible to observe and measure the geometric attitude of quartz veins, and of their deformation structures (boudinage, folds and stretching lineations). The measurements collected in this work were taken with a geologist's compass or with the *Fieldclino* mobile phone app.
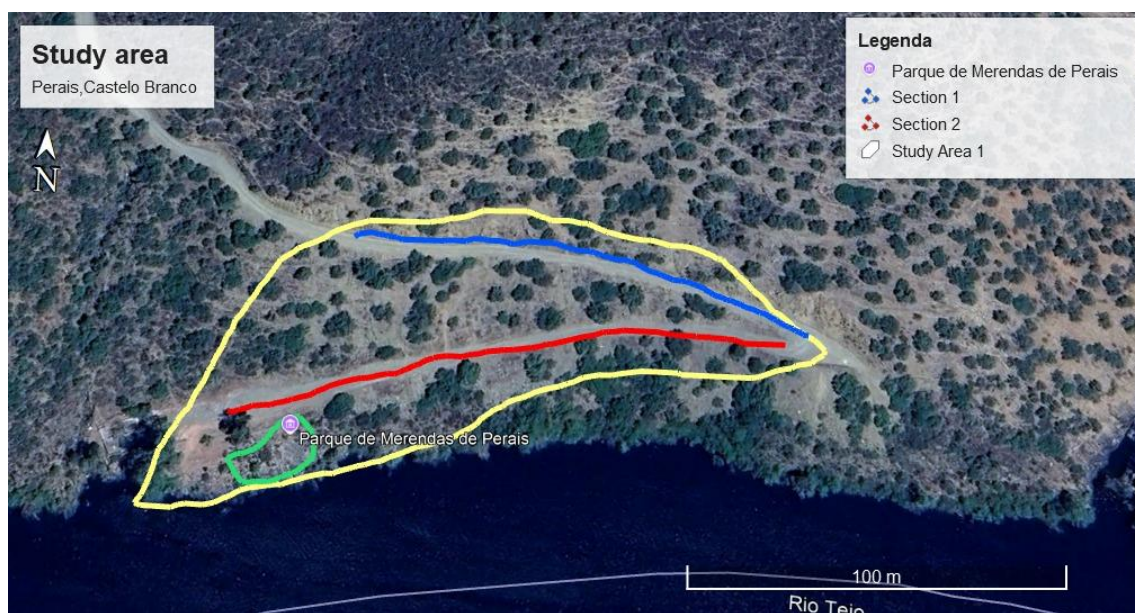
Figure 4.1 – Aereal photograph of the Study Area, with location of the geological sections in red and blue and the detail map area within the green line.

4.1.2 Detail mapping of geological structures

Another important method of gathering information in the field is geological mapping as it allows the projection of structures from a top view. Like cross-sections, mapping is important to identify the different lithologies, the structures that affect them and to plot the spatial distribution of the tectonic fabrics.

In the study area, in addition to the two road sections, it was selected an outcrop in the Tejo riverbed to produce a highly detailed structural map of the fabrics affecting the Malpica do Tejo Formation in this sector (Figs. 2.1C and 4.1). A top view of these structures is complementary to the cross sections as it will give a general three-dimensional perspective of the deformation. To create this detailed map, a grid with 2.5 by 2.5-meter cells was set over the exposure to allow a more accurate mapping of the selected area as shown in Figure 4.2.

Figure 4.2 – Aspect of the 2.5 by 2.5-meter subdivision of the grid set on top of the studied Perais riverbed outctops.

4.1.3 Oriented samples

The careful selection of oriented hand samples to produce oriented thin sections for microtectonics studies, is an important stage in structural geology to preserve the original orientation of the fabrics in the deformed lithologies and correctly define the style and kinematics of shear-zone-related structures in an exposure.

Oriented sampling starts with marking of the main foliation and stretching lineation attitudes in the sample itself in the outcrop position (Fig. 4.3). These marks are used to produce two perpendicular rock slices that are orthogonal to the main foliation, one that is parallel to the

stretching lineation (along the main tectonic transport direction) and defined as section A, and the other defined as section B, which is perpendicular to A and to the stretching lineation. The objective is to have a three-dimensional view of the tectonic fabrics and to check for multistage deformation evidence that can be otherwise of difficult identification in the field and in hand specimen. Both rock slices, A and B, are referenced with the field indications of the measured fabrics and physically marked with a small cut to keep the original orientation of the sample (see Fig. 4.3 A and B). These marks are used to produce oriented thin sections to correctly characterize the kinematics of the mylonitic fabrics that are typically formed along ductile to brittle-ductile shear zones.

Since this work aims to see whether the structures formed along a shear-zone developed in the Malpica do Tejo Formation are the result of one or several non-coaxial or coaxial deformation events, it is important that the sampling keeps the original orientation of the fabrics affecting the quartz veinlets of the Perais outcrops.

Figure 4.3 – Example of oriented sample collected in Perais picnic area. A) – Sampling with the orientation of main fabrics and the location of rock slices A and B; B) – Sample with orientation references in the rock preparation laboratory to produce the rock slices and respective thin sections.

4.2   Laboratory/Cabinet Work

4.2.1   *Preparing and analyzing thin sections*

The thin sections come from the samples collected during the fieldwork. Since the samples are oriented, the thin sections are produced to preserve field orientation. Thin sections are made in two perpendicular directions, A and B, as described above, which allows the identification of structures in three dimensions. The samples were cut with a diamond saw into oriented rock slices and these were used to produce the thin sections that were systematically observed under a transmitted light petrographic microscope to characterize the textures and identify the mineral associations that compose the tectonic fabrics. Representative areas of the thin sections were photomicrographed to document the most important mineralogical and textural aspects. The

textures and structures are described in the context of microtectonics, where a kinematic path that the rock may have undergone is proposed. After a detailed analysis of the thin sections, they will be placed in the light of a wider geological context of this region.

4.2.2   Photo interpretation

When conducting fieldwork, one important technique for data collection involves the use of a photo report. To complement the observations and measurements done in the studied geological cross sections and in the detailed mapping area, the collection of photographs aims to capture a comprehensive record of geological structures. Once the photographs are obtained, they undergo interpretation using a drawing software like Adobe Illustrator (commercial) or Inkscape (opensource). This process entails identifying and marking various geological structures such as folds, boudinage, foliations, lineations, quartz vein geometries, and faults. It involves interpreting the cross-cutting relationships of these structures and then proposing a relative timing (chronology of formation) and kinematic analysis of each structure type to understand how these geological features were formed. Although this is a job not directly done in the field it is dependent on the field observations, complementing important information collected in the field notebook.

4.2.3   Stereographic projection and structural analysis

Stereographic projection allows the plotting of linear and planar elements in a spherical surface using a Wulff (equal angle) or a Schmidt (equal area) stereographic net. Its application in structural geology is very relevant as it allows the projection of measured fabrics like lineations and foliations collected during field work, being very useful to have a big picture of the distribution of the different stage deformation evidence and to make statistical procedures that allow the identification of major structures and the reconstruction of early fabrics and primary features, such as bedding planes, in an equal area, lower hemisphere projection. This is a very important tool and a well-tested methodology to use in structural analysis, as it highlights the role of the deformation regimes that affect a specific region specially those under the influence of shear zones and multiply deformation stages. Stereographic projections of tectonic fabrics allow regional and local structural analysis as it can incorporate large amounts of data collected for regional geological mapping for instance, or to evaluate the possible deformation regimes associated with folding, buckling or tilting of primary structural elements along a cross section. In this work, stereographic projections of the measured fabrics were made using the Stereonet 11 software for Windows by Rick Allmendinger, available for download at https://www.rickallmendinger.net/stereonet.

5.   General concepts of structural geology and microtectonics

This chapter contains important concepts that are essential to understand field and laboratorial (microtectonics) data and will be used for the discussion on the evolution of the deformation in the Perais outcrops and to reinforce the conclusions presented in this thesis.

5.1   Flow

The term "flow pattern" refers to the velocity vectors of moving material particles. It can be either homogeneous or heterogeneous. The most observed type of flow is heterogeneous, as its pattern varies from one place to another, resulting in non-uniform deformation. Although the movement

of a particle is not independent, the flow in nature is generally heterogeneous. However, it depends on the scale of observation because when analyzed at different scales,an globally heterogenous deformation is possible to be individualized in sub-zones of homogenous deformation.

However when the deformation is homogeneous the "flow pattern" mantains the same independent of the observing scale(Passchier and Trouw, 1996).

5.2   Deformation

Deformation is the transformation from an initial to a final geometry by translation, rotation and/or volume change influenced by a determinate the given strain and stress that it is submitted to(Fossen, 2010). Strain is also part of the broader concept of deformation (which includes rotation, translation and expansion in a generic direction in addition to strain). Stress is not part of deformation but corresponds to the stress that causes it. In other words, the materials in question (rock in this case) respond or adapt to a stress by deforming themselves (including through an accumulation of strain or distortion).

Deformation is dependent on the position through time of the three principal stress directions that are defined, from major to minor, as σ_1, σ_2 and σ_3 . It can be subdivided into homogenous and heterogeneous (or inhomogeneous) deformation depending on 3 factors: the geometrical changes of area compared to the original shape, the relation between strain marker lines, and their angular relationship(Fig. 5.1).

Deformation can also be considered as coaxial or non-coaxial

The deformation can be coaxial or non-coaxial depending on the so-called vorticity of the strain flow (experessed by the kinematic vorticity number w_k). Coaxial deformation implies that the orientation of both the instantaneous, and finite principal stress directions are maintained equal (i.e., unchanged) from the initial to the final stage of deformation, implying that the kinematic vorticity as whole is zero $w_k = 0$. Non-coaxial deformation implies a progressive rotation of the principal stress directions as strain accumulates, resulting in a lack of coincidence between the axis of the instantaneous stress ellipsoid and the finite stress ellipsoid, which express a non-zero kinematic vorticity.

Starting with an orthogonal 2D or 3D grid, homogeneous deformation implies a final grid where the considered strain marker lines or planes are straight and parallel, making an angle with their equivalents in the undeformed original state, but maintaining congruent angular relationships between themselves: i.e., all original angles α in the undeformed state are congruently transformed in a same final β angle in the end state. This can also be represented by an original circular/spheric shape that transforms into an ellipse/ellipsoid (2D/3D, respectively) shape in the final geometry.
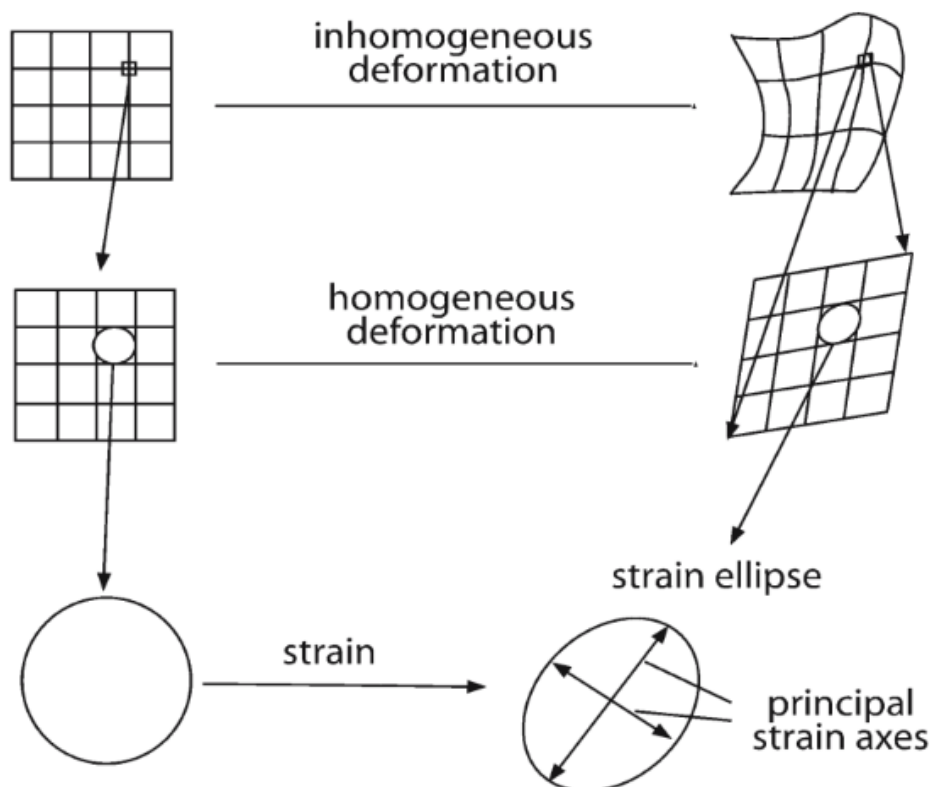
Figure 5.1 – Representative scheme to explain heterogenous deformation and homogenous deformation on a grid and on a circumference. Taken from Passchier and Trouw (1996).

Homogeneous flow has thus the following characteristics: instantaneous stretching axes (ISA) that represent the directions along which stretching is maximum and minimum are orthogonal in are orthogonal to each other.

If the stretching axis is symmetrical with the zero stretching rate axis, representing the direction along which there is neither stretching or shortening, then there is no area change in the flow, and this is dubbed isochoric and orthogonal.

When we have a reference frame fixed to the ISA and the angular velocity curve is symmetrical to the 0 angular velocity axis means that there is no rotation of matter involved in the flow (zero cinematic vorticity WK=0) and the zero angular velocity lines are orthogonal. In this case the flow is called coaxial due to the parallelism of the lines to the ISA. It displays an orthorhombic symmetry, and if there is no change in area/volume it is called *pure shear*.

If all the lines in the material endure extra angular velocity, we have dextral or right-handed rotation; or if it rotates we have sinistral rotation. In these two cases, the flow is non-coaxial because the strain marker lines are no longer parallel to the ISA, expressing non-null kinematic vorticity.

When the angular velocity curve is not touching the angular velocity axis then there is only one ratio line, so we have pure shear flow.

5.2.1 *Homogeneous and heterogeneous deformation*

Homogeneous deformation of a rigid body occurs when the grid reference lines keep their parallelism and the response to stress and strain is evenly distributed. On the other hand, heterogenous or inhomogeneous deformation occurs in heterogenous bodies where the different mineral compositions or rheology (e.g. combination of phyllosilicates and nesosilicates) lead to different responses to deformation, producing unevenly deformed reference lines with wavy and

sometimes warped shapes, depending on the angular relationships of each material with the stress vectors and their distance to the source of deformation.

Homogenous deformation can be produced under two forms of shear, by pure shear or coaxial deformation, or by simple shear or non-coaxial deformation. Inhomogeneous deformation occurs by the combination of both types of shearing.

5.2.1.1   Pure Shear

Pure shear occurs during coaxial deformation. It produces orthorhombic flattening of a rigid body by modifying the distance between the reference grid lines or planes while maintaining their original parallelism and angular relationships, as well as the orientation of the initial deformation conditions with unchanged principal stress directions (σ_1 to σ_3) and unchanged area/volume.

5.2.1.2   Simple Shear

In simple shear the parallelism of the reference lines and planes are preserved, changing the original angular (orthogonal) relationship between them, producing different dislocations from the origin. In this style of deformation, the maximum and minimum compression vectors change during time with a strong rotational, or non-coaxial, regime. Incremental deformation forces the delineating axes to rotate towards the main shear plane (fabric attractor). In this type of homogeneous deformation the area/volume is also maintained constant.

5.2.2   Progressive and finite deformation

A homogeneous creep pattern leads to an accumulation of homogeneous deformation. The stretch and rotation depend on the type of creep and are identified by the stretching and rotation of the lines. If the deformation is accumulated by pure shear creep we have an orthorhombic symmetry in the distribution pattern of the material with a different deformation history, also known as coaxial progressive deformation.

Simple shear leads to non-coaxial progressive deformation in which the distribution has a monoclinic symmetry. If the deformation is homogeneous at all scales, no evidence of progressive deformation can be found, but in the case of heterogeneous deformation it can be found. Pure shear and simple shear produce different structures, and it is the monoclinic fabric that allows us to determine them. If the deformation is homogeneous, you can move into three dimensions and go from a representation of representation to one of 9 in matrix style. 3 of these numbers correspond to stretching rates; three correspond to vorticity and magnitude and 3 correspond to orientation.

5.3   Fabric

Fabric is the designation used for a geometric configuration of elements or mineral texture in a rock. The fabric can be primary or secondary. A primary fabric corresponds to an original rock texture without the influence of later geological events, like bedding in sedimentary rocks or the mineral preferred orientation defining a magmatic flux in plutonic or volcanic rocks.

Secondary or tectonic fabrics are produced during deformation. It is present in many forms and created by different deformation and metamorphic conditions. Tectonic fabrics can be either linear, planar, or plano-linear depending on the mineral that defines it, and the intensity of the deformation regimes submitted to a rock.

5.3.1 Foliation

Foliation is a continuous and pervasive planar mineral texture in a rock that is formed during primary or secondary processes. A primary foliation is formed during sedimentary or magmatic processes. In sedimentary rocks, it encompasses bedding, crossed bedding, hummocky laminations and other planar textures that were produced by rhythmic succession of beds of different granulometries, which gradually or dramatically separates coarser grained sediments from fine grained debris. In igneous rocks, a magmatic foliation can be the product of the mineral array marked by mafic and felsic minerals, such as banded cumulates formed in the context of a magmatic chamber by fractional crystallization, by the alignment of phenocrysts and mafic minerals by the flux in a magmatic chamber or during the emplacement of plutonic rocks, and it can be the product of volcanism when subaerial or subaquatic extrusion of lavas or tuffs physically separate the mineral components in layers forming planar arrays, in a similar way as sedimentary rocks.

Secondary foliations are formed as the result of deformation and metamorphism (Fig. 5.2). These foliations generally have an overprint pattern of primary foliations and even to other secondary foliations. They can be produced by folding, being parallel to the fold axial planes (in pure shear), or along shear zones (in simple shear), forming C-S and C'-S shear bands. In both cases, the foliation is perpendicular to the main compression (σ_1) that produces the deformation. These are important to decode the tectonic and metamorphic evolution of a region. When secondary foliations are generated, they are often associated with ductile deformation of a rock, but they also develop in brittle conditions. Defining secondary foliations is not straightforward, as they can be difficult to distinguish from primary foliations when fabric transposition occurs and new arrays of coarse-fine grained minerals are tectonically formed under high to low metamorphic conditions. Secondary foliations have different morphologies such as cleavage, schistosity, crenulation and banded.
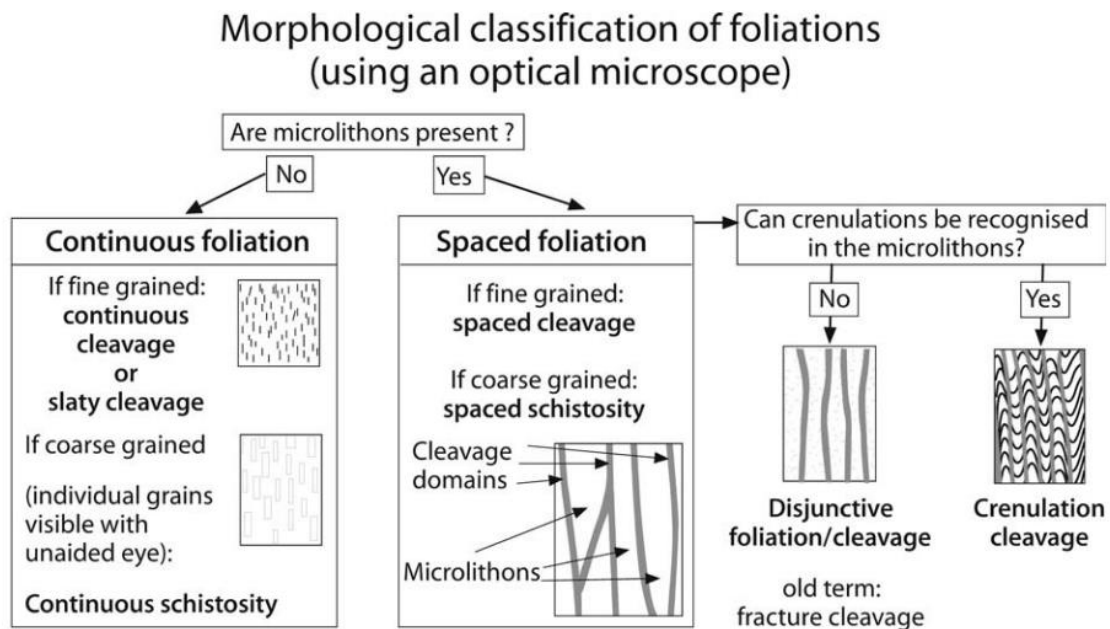
Figure 5.2 – Representative scheme of different types of foliations and how they organize. Taken from Passchier and Trouw (1996).

5.3.1.1 Continuous Foliation

Continuous foliation is constituted by a homogeneous distribution of planar minerals as in the

case of phyllosilicates that are organized perpendicularly to the main compressional direction. If these minerals are coarse grained and visible to the naked eye, it is called schistosity. If these minerals are only visible microscopically, it goes into the definition of cleavage or slaty cleavage.

5.3.1.2   Spaced Foliation

A spaced foliation produces two domains, cleavage and microlithons. The cleavage domains are planar and anastomosed and contain planar minerals, usually micas, which are sub-parallel to these domains. Microlithons are located between the cleavage domains and contain weak preferential orientations and are usually formed by polygonal minerals such as quartz and feldspar. Past foliations can be preserved in microlithons. They can be subdivided based on the structure of the microlithons. If they contain microfolds or fold hinges of a previous foliation (primary or secondary), they are called crenulation cleavage and the microlithons assume the name of crenulation cleavage domains. These fold hinges are separated by a new set of spaced cleavage developed in the limbs of the microfolds, allowing the complete transposition of the old fabric by the newly formed. If they do not contain relics of these micro folds, they are called disjunctive cleavage. The morphology of crenulation cleavage depends on several important factors such as lithology, temperature, and intensity of deformation, which influence the final morphology. A special type of spaced foliation defines a layered composition, where the microlithons and cleavage domains are continuous enough to resemble a layer that mimics a primary foliation (bedding). Foliations can be modified in different ways during deformation. The rheological contrast between different planar and polygonal minerals produces mechanical contrasts during deformation, generating small deformation bands characterized by high strain. The less competent minerals tend to accumulate more deformation along the bands, leading to layers limiting the most competent mineral assemblages.

5.3.2   Tectonic lineations

Tectonic lineation is a pervasive linear mineral arrangement formed by rock deformation. There are two types of lineation: object lineation, which is a three-dimensional feature developed by syn-tectonic mineral growth, and trace lineation that is produced by the intersection of at least two foliation sets (primary and/or secondary). The first type includes stretching lineation, which is formed by the increased deformation along a shear zone, and it is parallel to the lower stress direction (σ_3) and perpendicular to sigma 1 and 2. Another case is the generation of slickensides formed along brittle conditions in fault planes or in the limbs of folds, and they are the result of the relative tectonic movement between two sliding blocks. In these situations, lineation is parallel to the tectonic movement, and it is useful to trace kinematic criteria that define a shear sense along shearing planes.

In the case of an intersection lineation, the combination of the two intersecting planes produces a line that also defines the main stretching direction (sigma 3), forming a pencil cleavage that is usually parallel to fold axes.

5.4   Rheology

Rheology is the study of how rocks respond to stress. When subjected to stress rocks can exhibit ductile (viscous and plastic), and brittle (elastic) behavior. Elastic behavior means the rock can return to its original state up to a certain stress (yield stress) producing brittle rupture. The ductile or plastic/visocus behavior in deformation is reached when a material continuously accumulates or adapts to the induced stress without recovery. Brittle behavior produces fractures, faulting and

cataclasis of individual mineral grains, leading to the milling of the original rock into increasingly smaller fragments producing fault gauges. Ductile or plastic deformation occurs when the materials are continuously deformed, as in the case of increasing temperature conditions during metamorphism when it involves higher rates of intra- and intercrystalline deformation during simple or pure shear. This type of deformation is not restricted to high metamorphic conditions, as it can occur in unconsolidated wet sediments or, in low metamorphic conditions in the case of carbonated rocks. Therefore, ductile deformation is directly dependent on the rheology of rocks and on the strain-rate applied (relationship between the stress tensors).

Any material undergoing stress initially exhibits an elastic behavior until it reaches plastic deformation. If the stress continues to be applied, plastic or permanent deformation occurs after the rock suffers the plastic yielding.

5.5   Pressure solution and Solution transfer

Pressure solution and transfer solution can modify an original grain geometry to de point of defining a secondary foliation. These processes leave a seam of insoluble material like oxides or micas along the dissolution surfaces that allow the recognition of stylolites or can often define a pressure solution cleavage. Stress-induced dissolution helps to develop foliations, with increased rotation of elongated and planar minerals synchronously with the preferential dissolution minerals such as quartz or carbonates.

5.6   Dynamic recrystallization

The dynamic recrystallisation and oriented growth of minerals is an important mechanism for the development of planar and linear secondary fabrics. This type of recrystallisation process occurs due to the increased applied stress and corresponding accommodated strain by rocks that forces original mineral assemblages to adapt to new tectono-metamorphic thermodynamic (P, T) conditions that results in new mineral shapes (intra-crystalline deformation). In the case of quartz and feldspars, the shape change forced by deformation leads to the creation of internal structures, that are identified in thin section by the formation of wavy extinction lamella, sub domains and their subdivision into small polygonal grains (sub grain rotation recrystallization) that rearrange the original shapes into new stretched ones, defining a compositional layering with a tectonic origin.

5.7   Shear zones

Shear zones and shear bands are areas where strain is accumulated through the tectonic movement, which separates rock blocks that show less deformation evidence (Fig. 5.3). This allows a strong inhomogeneous behavior of deformation within regions where shear zones are present enhancing the way the different mineral components react to deformation.

Shear zones and shear bands characteristics are dependent of pressure and temperature conditions, which influence the type of tectonic flow and the rheology of the mineral assemblages in a rock. The shear zones can be classified as brittle, brittle-ductile, ductile-brittle and ductile according to the main deformation regime that affects a specific rock.

5.7.1   Brittle shear zones

The brittle character of a shear zone is defined by the propagation of faults and fractures in rocks,

taking advantage of previous weakness that the rock already had. This produces an array of intricate planar structures that leads to the gradual diminishing of grain size by crushing that generates larger volumes of milled rocks as deformation accumulates along the main propagation zone. This process creates different types of fault gauges or breccias that can be defined as follows.

5.7.1.1 <u>Non-cohesive fault rocks</u>

Non-cohesive fault rocks are generally found in the shallower segments of shear zones or faults where participation of mineralizing fluids or processes is neglectable. These unconsolidated rocks occur in fault zones of different thicknesses and can be subdivided into non-cohesive breccia, non-cohesive cataclasite and fault gauge.

5.7.1.2 <u>Cohesive fault rocks</u>

Cohesive fault rocks can be divided into cohesive breccia, cohesive cataclasite, pseudotachylyte and tachylyte. While the first two types of cohesive fault rocks are formed by rock fragments milled along brittle faults and consolidated by chemical cements (iron oxides, carbonates, siliceous solutions), pseudotachylytes and tachylytes are rock faults formed by local melting of the rocks leading to a glassy obsidian-like cement that surrounds fine- to coarser grained broken rock fragments.

5.7.2 Mylonites

A mylonite is an intensely deformed rock that shows evidence brittle-ductile to ductile deformation regimes (Trouw et al., 2010). It occurs in very high strain regions in metamorphic conditions ranging from greenschist to granulite facies metamorphism (Fig. 5.3). Mylonites are classified according to the metamorphic grade and intensity of deformation at which they were deformed, according to the associated mineralogy or according to the deformed matrix/porphyroblast ratio. The deformed matrix–undeformed rock ratio classification of mylonites ranges from protomylonite when the matrix is between 10-50% of the bulk rock composition, mesomylonite if the matrix is 50% to 90%, and ultramylonite when the matrix composes more than 90% of the bulk rock.
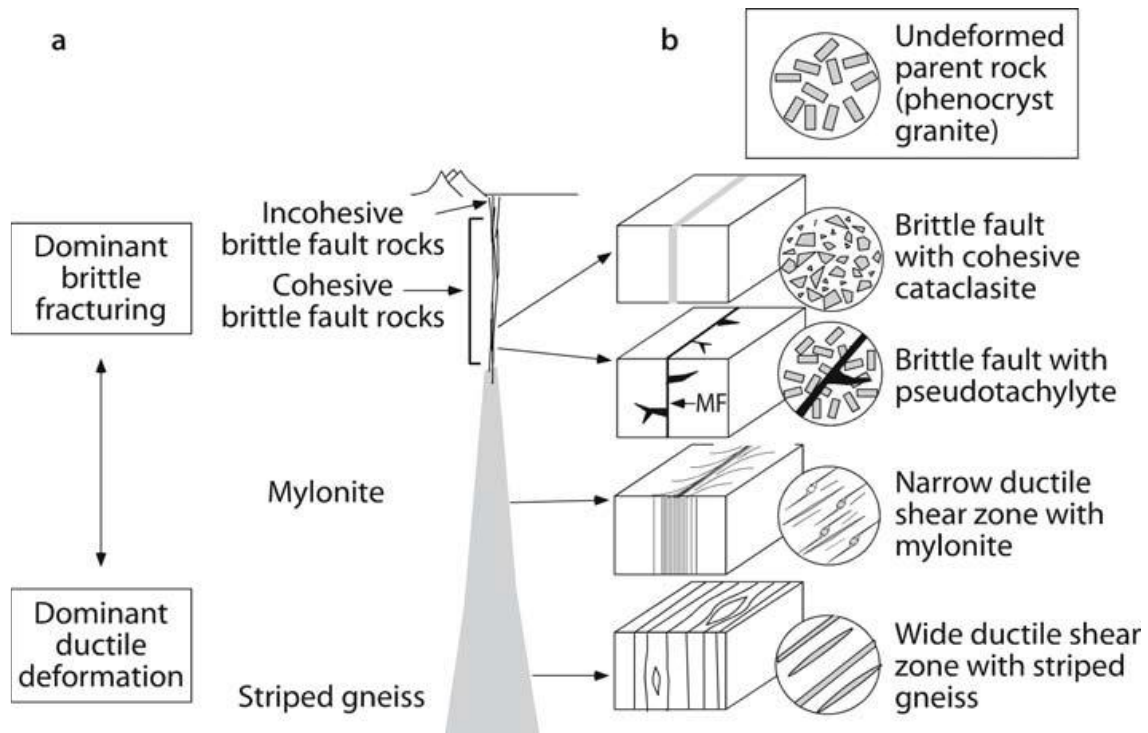
Figure 5.3 – Distribution of the main types of fault rocks with depth in the crust in a schematic cross-section through a transcurrent shear zone. Taken from Passchier and Trouw (1996).

Mylonites may contain porphyroblasts, large-sized metamorphic minerals or blasts that stand up from the average size of the minerals composing the mylonitized matrix, which can be used as tracers of the deformation within a metamorphic rock. Porphyroblasts can be classified as pre-, syn-, inter- or post-kinematic according to their relationship with the minerals defining the matrix and the fabric inclusion trails preserved within the porphyroblasts (Passchier and Trouw, 1996) (Fig. 5.4). On the other hand, the term porphyroclast is used to define relict minerals or mineral aggregates that survived the mylonitization process and give important information on the previous history of the protolite (or precursor) rocks (Fig. 5.5). In both cases, the neoformation of these elements in mylonites is because of the difference in rheology they present in respect to the deformed matrix.
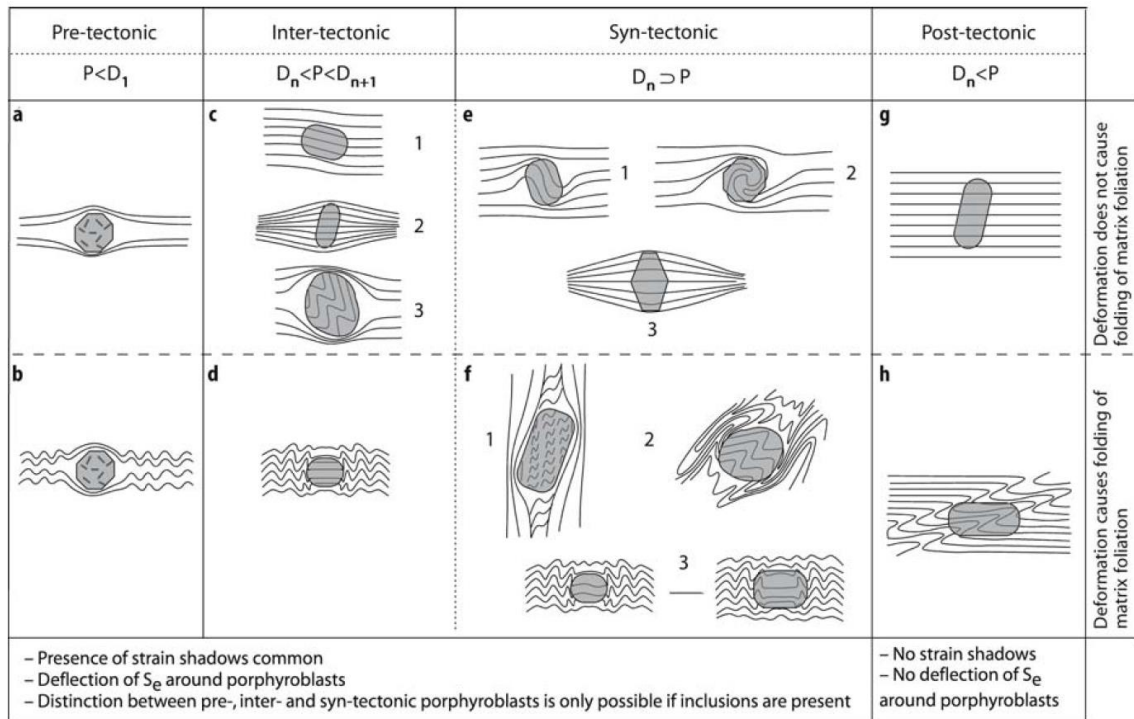
Figure 5.4 – Porphyroblast-matrix relationships. Taken from Passchier and Trouw (1996).

The planar elements in a mylonite are called mylonitic foliation and the linear fabrics are called aggregation lineation. Aggregation lineation is more common in polymineralic rocks where there has been a considerable grain size elongation. Mylonites contain two or three foliations that are angularly associated with each other and that developed contemporaneously and sometimes overlap. These foliations are usually subject to sin-kinematic folding, forming isoclinal intrafolial folds that are contemporary with this foliation. Some of these folds can generate sheath folds that are parallel to the tectonic transport, as these folds have a tubular shape, and others are cylindrical folds with axis parallel to the stretching/transport lineation. The amplitude of these folds is variable and tend to reduce in size with increasing strain.

Mylonites have diverse and specific geometric characteristics depending on the orientation of the observed section (Fig. 5.5). In sections perpendicular to the foliation and to the lineation, the rock shows orthorhombic symmetry, and primary aspects could be traceable. The section perpendicular to the foliation and along the stretching/transport lineation is more adequate to identify monoclinic shear indicators such as sigmoid and deltoid shapes of porphyroblasts/clasts, C-S and C'-S shear bands, asymmetric folds, tectonic fish and bookshelf structures in micas or in competent materials/layers (Figs. 5.5a-j and 5.6). Another aspect of mylonites is that its characteristic structures rapidly disappear away from the main shear zone and structures symmetry is more evident, as expected in inhomogeneous non-coaxial deformation.
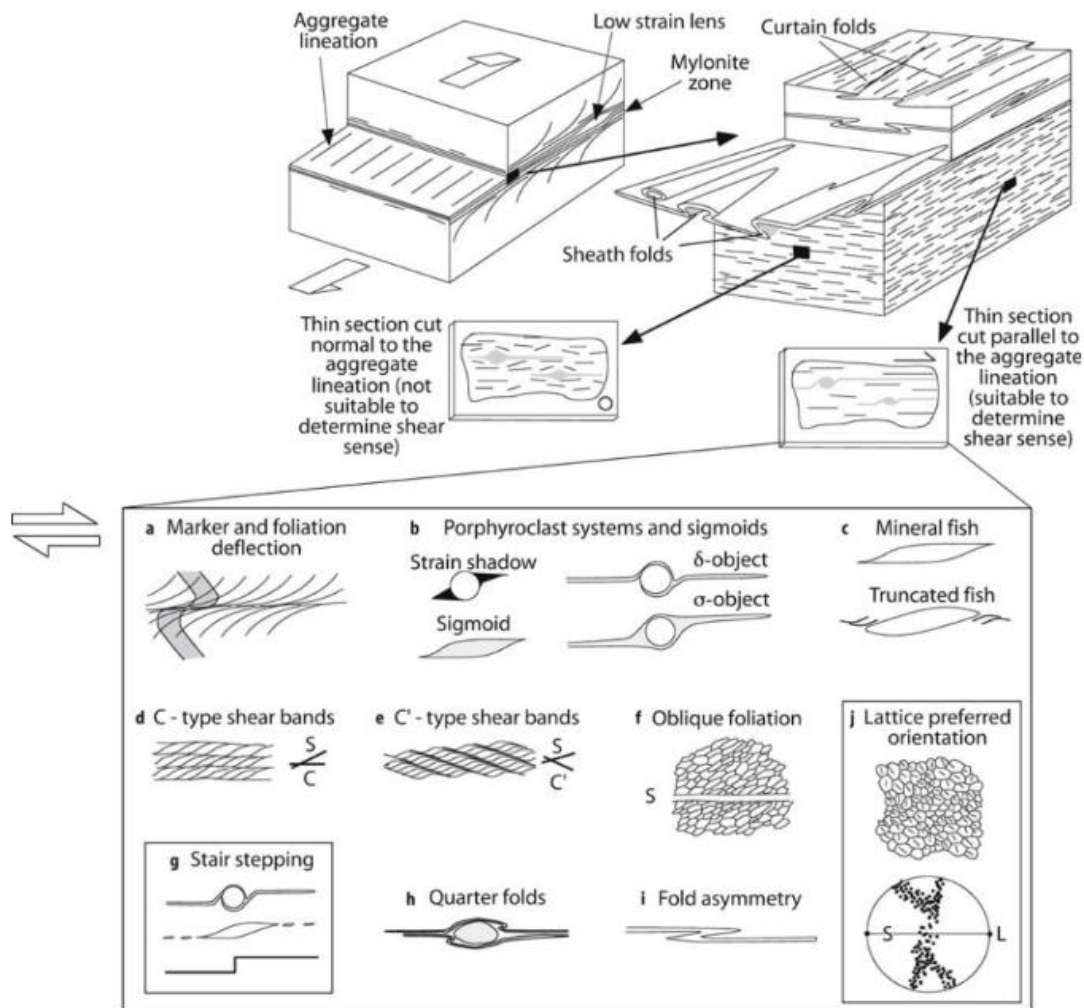
Figure 5.5 – Scheme exposing the different mylonitic elements and their association in a bigger scale. Taken from Passchier and Trouw (1996).

5.7.3 Shear band cleavage

Shear zones are composed of smaller scale shear bands. There are two main types of shear bands: C-S and C'-S. In both cases they are related to the development of a foliation (S) that is oblique to the main sliding plane (C or C'), which becomes increasingly parallel as simple shear deformation accumulates in the shear zone (Fig. 5.6). C and C' type shear bands dispose regularly in a mylonite with spacing becoming tighter with grain size of the protolite rock and with increasing deformation. S planes are parallel in both shear band types and are perpendicular to the main compressional vector. The relationship between C, C' and S planes give indications on the kinematics of the shear zone, with C planes parallel to the main deformation zone. C' planes are also called as extensional crenulation cleavage (ecc) and as the name suggests, they have an extentional/thinning behavior, allowing the late deformation stages of a shear zone to produce asymmetric boudinage (false boudin-like structures) as response to the accommodation of strain along a shear zone. C' planes frequently cut early C-S planes and enhance the relationship between strain and stress, increasing the rotational component along shear zones.

20
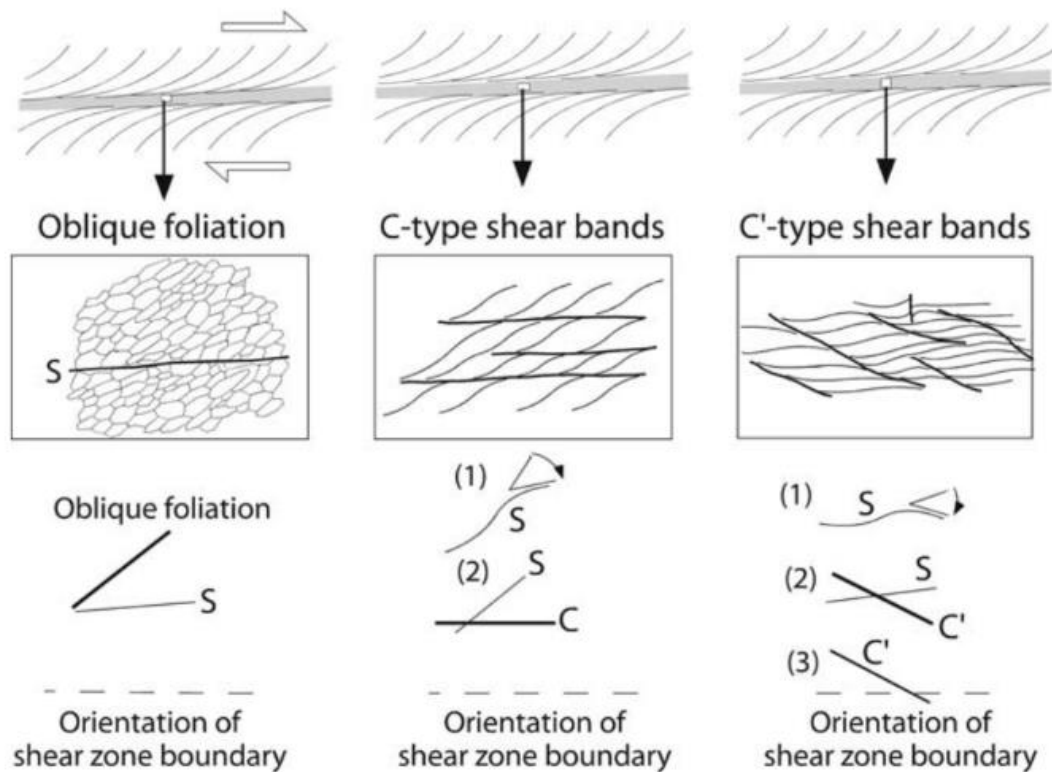
Figure 5.6 – Scheme representing the different patterns possible to obtain in shear bands. Taken from Passchier and Trouw (1996).

5.7.4 Sigmoids, deltoids and mineral fishes

A sigmoids, deltoids and mineral fishes are a micro to macroscale structures that are formed by simple shear.

Sigmoids present sigma (σ) shapes that are developed in shear zones as consequence of the kinematics along the shear plane. In microtectonics, a sigma structure is characterized by a monoclinic and approximately rhombic shape with two tails of recrystallized mantle that lay at both sides, above and below, the shear plane of the rigid body (porphyroclast or porphyroblast), because of the kinematics along a shear band. The position of this mantle is because is formed in the pressure shadow of a rigid body during simple shear, allowing the gradual drag of the tails along the shear band indicating the kinematics along the transport lineation (Figs. 5.7 and 5.8).

Similarly, deltoids have delta (δ) shapes and are also formed during non-coaxial general shear along a ductile shear zone. In this case, a delta shape in a shear zone is developed by a strong rotational component of a rigid body and the surrounding mantle, which includes the S foliation. The rigid body rotation is concordant to the kinematics along the shear band and drags the S planes and recrystallized mantle tails synchronously, towards an upright or passing this position. Geometrically, a delta shape is also monoclinic with its recrystallized tails wrapping around the rigid body like a snowball in a position above and below the symmetry line leaving a depression or embayment due to the rotation of the clast/blast (Fig. 5.8).

Mineral fish, which are frequently found in mylonites, are long lozenge or lens-shaped isolated crystals. Their longest dimension is typically positioned at a little angle to the mylonitic foliation and are good indicators of shear band kinematics (Fig. 5.7). The most prevalent are mica fish, which are mineral fish of big, isolated white mica crystals found in micaceous quartzitic mylonites. Typically, individual mica fish with distinct stair stepping have trails of tiny mica

21

fragments that continue into the matrix from their tips.
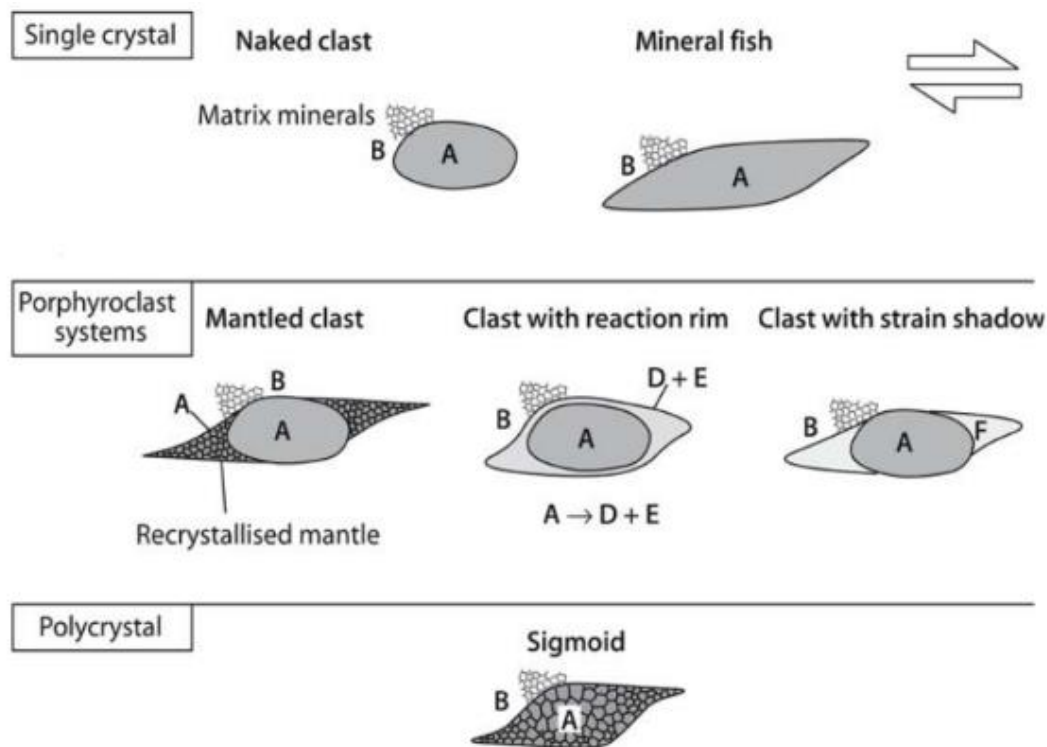
Figure 5.7 – Scheme of genesis of different types of sigmoids. Taken from Passchier and Trouw (1996).
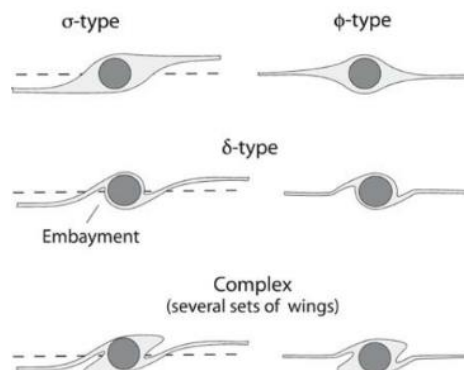
Figure 5.8 – Representation of sigmoid and deltoid shapes and their tails of recrystallized mantle. Taken from Passchier and Trouw (1996).

5.8   Boudinage

Boudinage is a geological process that reflects the mechanical contrast between materials with different rheologies. It consists of necking and stretching of a rigid planar marker or layer within a more plastic/viscous or less competent matrix. Their differential accommodation behavior to an imposed tectonic stress allows the partitioning of the reference rigid layer into smaller brittle segments, while the matrix adapts plastically to the separation of each segment. Boudin geometry is dependent on the primary position of the rigid layer in respect to the stress field and will rotate towards a final position. This rotation enables different kinds of separation that will characterize the nature of the shear regime (simple or pure), being sometimes aided by the presence of conjugated extensional shear zones (e.g. C'-S). Also, the rotational component in boudinage may lead to the formation of domino type boudins that asymmetrically adapt to the induced stress and

may represent different stages of extensional and compressional regimes during the layer rotation from the initial to its final position, in terms of its relationship with the stress directions (Fig. 5.9). Asymmetrical boudins occur in sedimentary or tectonic units and are useful for determining the direction and kinematics of a shear zone. There are two types of asymmetrical boudins: Shearband boudins which present a long and curved lenticular shape that is arranged where the top of its lenticule tends to tip over into the next boudin, and domino boudins which have an angular shape and their interbody surface slopes towards the next boudin.
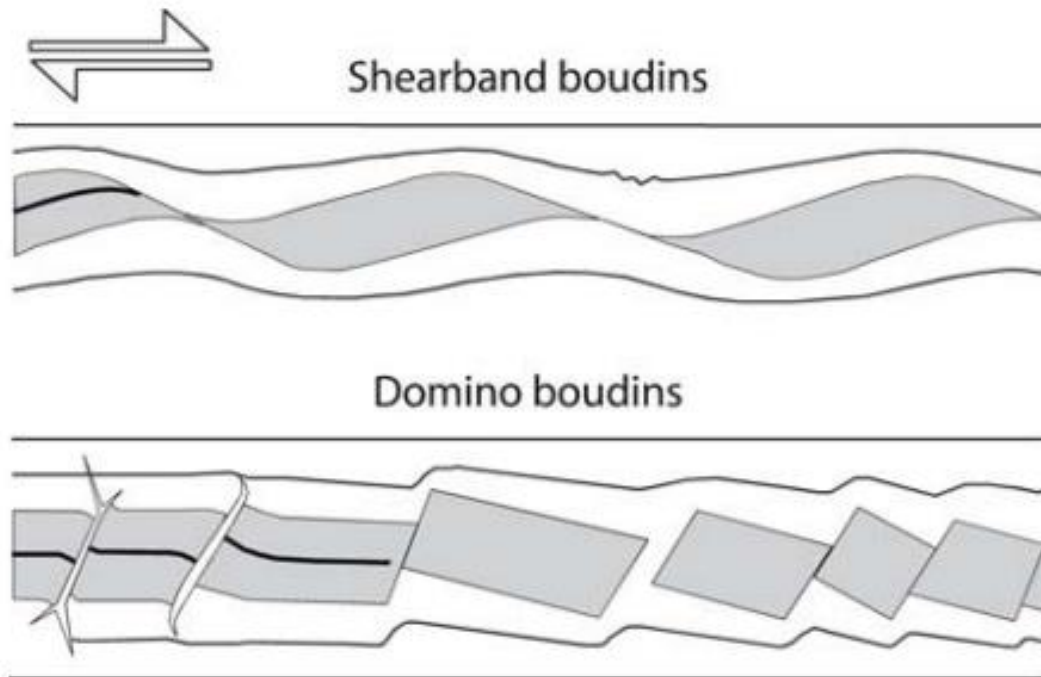
Figure 5.9 – Scheme representing the different types of boudin in different rheological contexts. Taken from Passchier and Trouw (1996).

6. Results

Based on the progress of the work, the attained results represent a significant step towards fulfilling the established objectives. The findings presented in this section enable the meso- to micro-scale identification of folding and boudinage patterns in the quartz veins and veinlets in slates and greywackes of the Malpica do Tejo Fm. in the Perais exposures.

6.1   Fieldwork

During the fieldwork, two centimetric-metric intercalated lithologies were identified in the studied cross sections and in the riverbed outcrop. The first lithology has a black to dark grey color and corresponds to slates in the chlorite-biotite metamorphic zone, where deformation is more evident with the main secondary foliation (S_n) completely transposing the bedding (S_0). The second lithology emerges in metric to centimetric layers that mimic the bedding and are composed of fine to coarse-grained greywacke showing a primary sedimentary texture and light grey to brownish colors. As in the first case, bedding is apparent, and it is transposed by the main foliation in the boundary with the slaty layers (Fig. 6.1)

Figure 6.1 – Folded quartz veinlet (in black) within fine-grained greywacke layer, evidencing total transposition of bedding (S_0) by the main foliation (S_n) (yellow line).

The three sectors studied in this work (Fig. 4.1) were important to have a 3D view on the structure of the Perais exposures. The main foliation (S_n) is generally very pervasive and transposes bedding, is axial planar of cylindrical intrafolial folds and surrounds metric boudins of greywacke composition. In this way, this work helps to define the compositional layering in the Malpica do Tejo Fm. that cannot be assumed as a primary fabric/foliation, and therefore it will be resumed as

a secondary and transposing $S_0//S_n$ foliation. This secondary foliation is also axial planar of the folds defined by the precocious quartz veins and veinlets that are more abundant in the finer grained metasediments. Also, there is evidence of latter, more brittle deformation events that allowed the vertical and horizontal waving of these fabrics, as well as latter stages of quartz veins and ribbons that cut the intrafolial folds of the precocious veins identified within the metasediments.

6.1.1 Cross section 1

Cross section 1 was made in upper part of the road leading to the Perais picnic area, where the deformed metasediments of the Malpica do Tejo Fm. are exposed (Fig. 6.2).
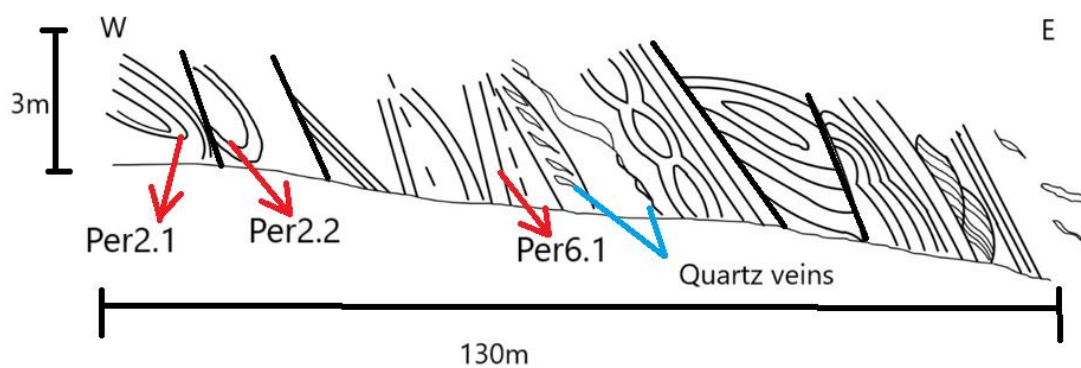
Figure 6.2 – Representation of cross section 1, in the upper part of the dirt road leading to the Perais picnic area with the localization of the collected samples used in the microtectonics study.

In this area the most competent greywacke layers define isoclinal folds and boudins. It was possible to locally identify mesoscopic shear bands affecting quartz veins and veinlets, with a main kinematics towards E, along a steep stretching lineation that is parallel to this cross section. Also, several brittle faults are cutting the previous ductile fabrics with a metric to decametric spacing, which are responsible for local bending and tilting of the structures.

The ductile structures identified are two consecutive synforms with the main foliation as the axial planar cleavage that also surrounds them. This foliation is inclined on an average of 70º to the northeast, and the fold axes are sub-horizontal to gently dipping towards the SSE (Figs. 6.2, 6.5 and 6.6). In the center of this cross section some en-echelon quartz-filled veins evidence a top-to-the east movement, which is concordant to the boudinage observed in the coarse-grained greywacke layers. To the east, the cross section presents several brittle faults and kink bands that seem to be related to the fault movements, producing the waving of the more ductile fabrics and the early quartz veins.

Figure 6.3 – Field aspect of one of the synclines represented in the westernmost sector of cross section 1. Dashed line represents main foliation that is axial planar to this fold and parallel to the fold limbs (isoclinal fold), transposing bedding in this latter situation ($S_0//S_n$).
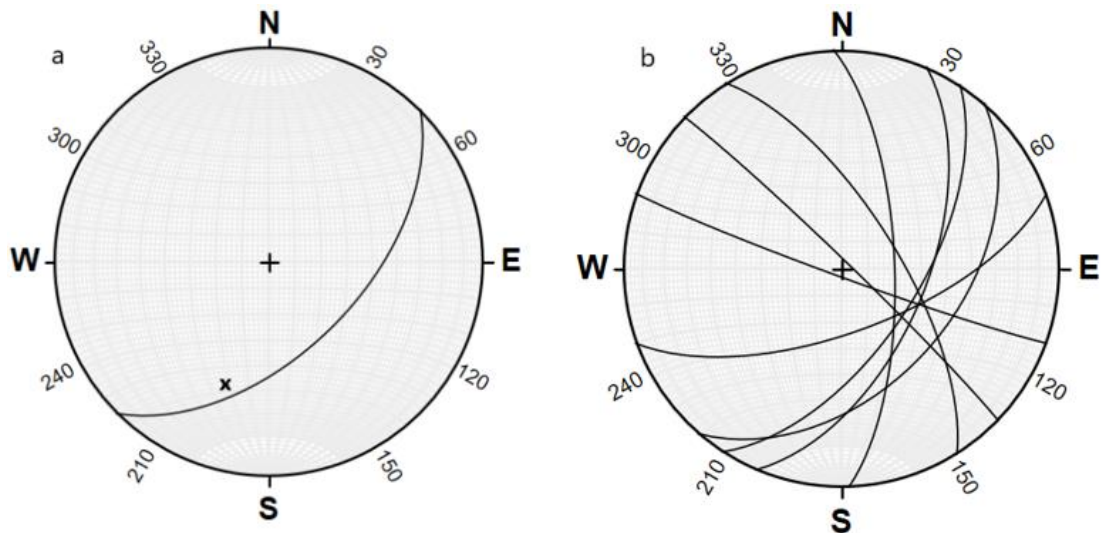
Figure 6.4 – Stereographic projections of the structural measurements in cross section 1. a) stereographic projection of the brittle fault plane between PER2.2 and PER2.1 and the point is the striae. b) stereographic projection of the foliation ($S_0//S_n$).

6.1.2 Cross section 2

Cross section 2 is almost parallel to the previous. It represents the lowermost road section of the dirt track leading to the Perais picnic area (to the west) (Fig. 6.5). Like in the previous case, a preferential subparallel orientation of the axial planes of the isoclinal folds and the main foliation is evident, with the transposition of the main foliation and bedding in the limbs ($S_0//S_n$). Several brittle faults are also present, showing similar orientations as in cross section 1. To the east, the main foliation ($S_0//S_n$) presents more gentle dipping (Figs. 6.5 and 6.6 and 6.7), probably related to brittle fault movements that allow the sub-horizontal folding of the ductile fabrics in the metasediments.
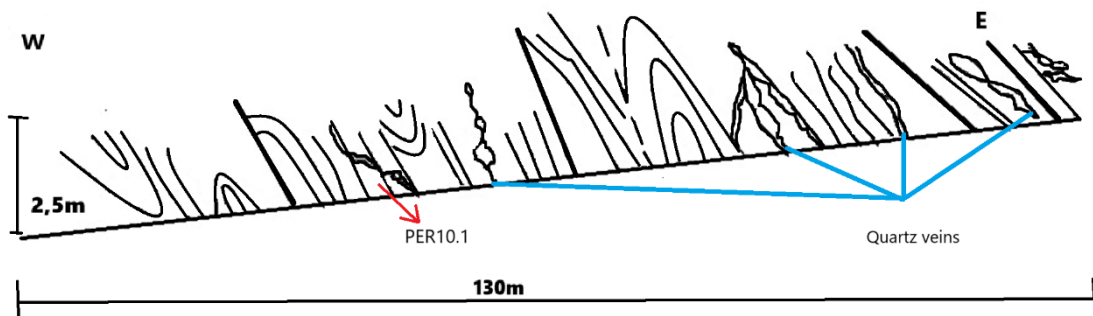
Figure 6.5 – Geological cross section 2 with the main structures and the location of the collected sample PER10.1.

In cross section 2, the lithologies appear to be slatier, showing, as in the upper sequence, folded structures affecting the coarser-grained metasedimentary layers, multiple generation quartz veins and brittle faults. Likewise, early folds have the main foliation parallel to the axial plane and are isoclinal (bedding transposed by S_n in the limbs). There are multiple generations of quartz veins including those defining en-echelon structures with top-to-east kinematics, intensely folded veinlets and post folding cross cutting veins, which present more straight geometries.

Figure 6.6 –Structural measures collected in the studied cross sections in the dirt track leading to the Perais picnic area.
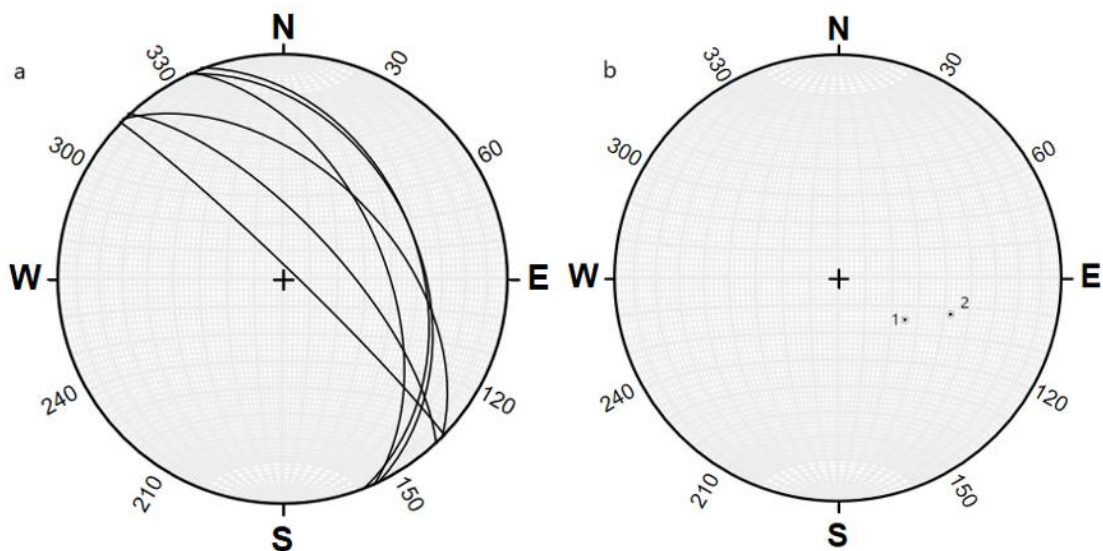
Figure 6.7 – Stereographic projections of the structural measurements in cross section 2. a) stereographic projection of the main foliation ($S_0//S_n$); b) stereographic projection of measured tectonic lineations. 1) corresponds to the axis of the crenulation cleavage and 2) corresponds to stretching lineation.

6.1.3   Riverbed exposure: detailed structural mapping

The detailed structural map made in the Tejo riverbed exposure (Fig. 6.7) shows different structures with important cross-cut relationships that complement observations made in cross sections 1 and 2. Dark-grey and blackish metapelites and greyish metasiltitic fine-grained metagreywacke rocks are the main rocks observed along this exposure. As in the previous case, primary sedimentary structures are not preserved, as they are transposed by a very pervasive foliation that obliterated them. The exquisite nature of the studied outcrop puts in evidence the ductile deformation that affected the Malpica do Tejo Fm., with synchronous emplacement of quartz veins and veinlets that show a complex array and geometries of folds and boudins, which are cross-cut by a series of brittle and discrete faults and "undeformed" quartz veins.

The main foliation is transposing bedding (S_0//S_n) and presents as a parallel cleavage, sometimes contouring the more siltitic layers, leaving almond shaped bodies of coarser grained rocks, where the foliation is oblique to the layer boundaries. In the more pelitic layers, the foliation is very pervasive and presents more abundant and thinner quartz veinlets that frequently show boudinage and intrafolial folds. These veinlets are thicker in the sandier layers and less pervasive. Nevertheless, deformation patterns are the same as in the pelitic ones, enhancing the synchronicity between both sets of deformed veins with deformation. As in the case of the studied cross sections, but with better exposure than the previous cases, the transposed bedding (S_0//S_n) is dipping between 70º and 90º to northeast. The stretching lineation measured in the quartz veins is 50-80º to ESE, which are sub parallel to the mesoscopic fold axis of the quartz veinlets (Fig. 6.8). Apparent dextral and locally left-handed kinematics of no-coaxial shear affecting these rocks are observed in this exposure (Figs. 6.8, 6.9, 6.10 and 6.11). However, because tectonic transport is parallel to the stretching lineation (almost orthogonal to the exposure), movement must be deduced obliquely to the outcrop. In this sense, a top-to-east kinematics synchronous with the development of S_n is observed, fitting with observations made in cross sections 1 and 2.
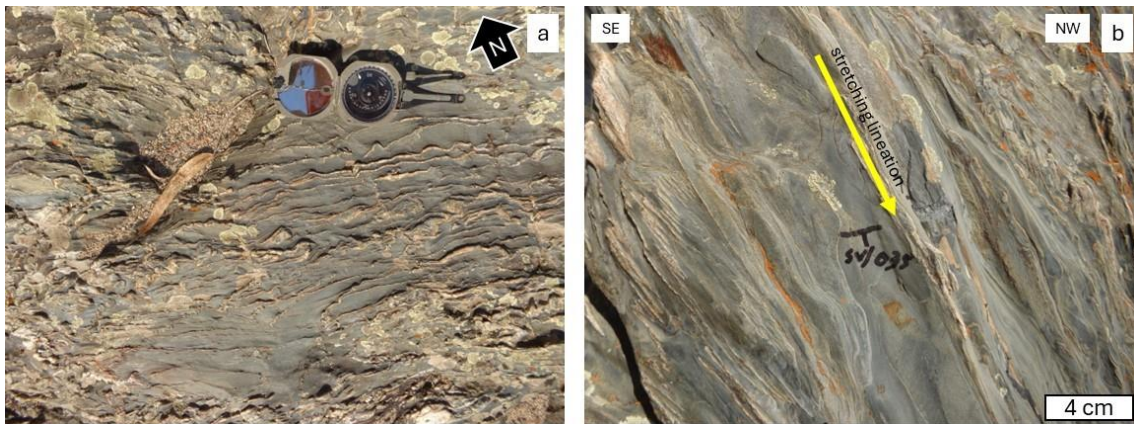
Figure 6.8 – Field photos of the exposures in the riverbed ot the Tejo river. a) (top view) quartz veinlets with intensive folding and boudinage, with apparent kinematics; b) (cross section) vertical foliation (S_n) and stretching lineation parallel to the fold axis in a). Sampling site of RIO-E1 oriented sample with orientation of the transposing foliation.

The ductile tectonic fabrics (S_0//S_n and early quartz veins) are cut by discrete N-S upright faults with an apparent dextral movement. Also, a second generation of upright quartz veins cut the entire outcrop and overprint the earlier ones with N-S orientation. They show straight geometries and are evenly distributed. There are late quartz en-echelon veins with apparent dextral sigmoidal shapes.
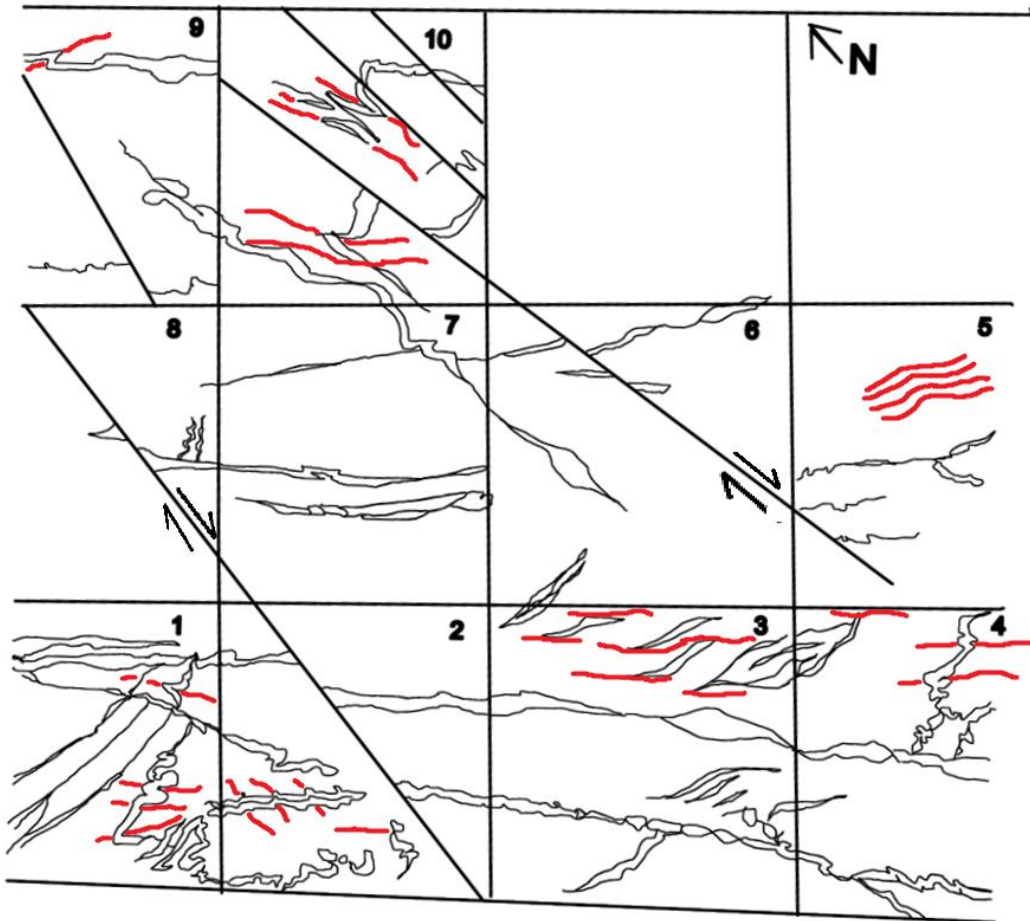
Figure 6.9 –Detailed structural map of the riverbed exposures. $S_0//S_n$ in red and faults and quartz veins in black.
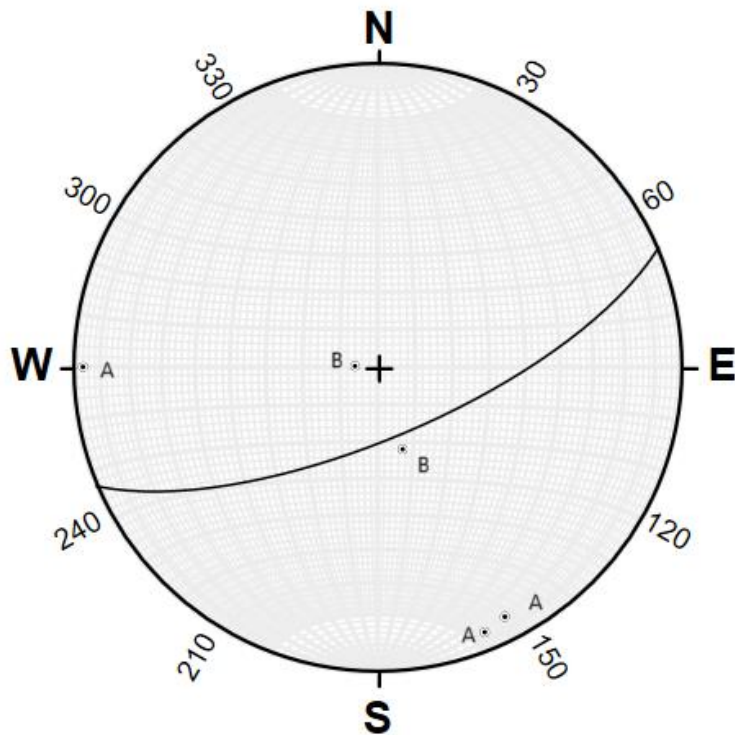
Figure 6.10 –Stereographic projections, the plane is a fault that crosses the area, A points are correspondent to the direction of one family of quartz veins and B points are correspondent to the axis of the quartz veins folds.
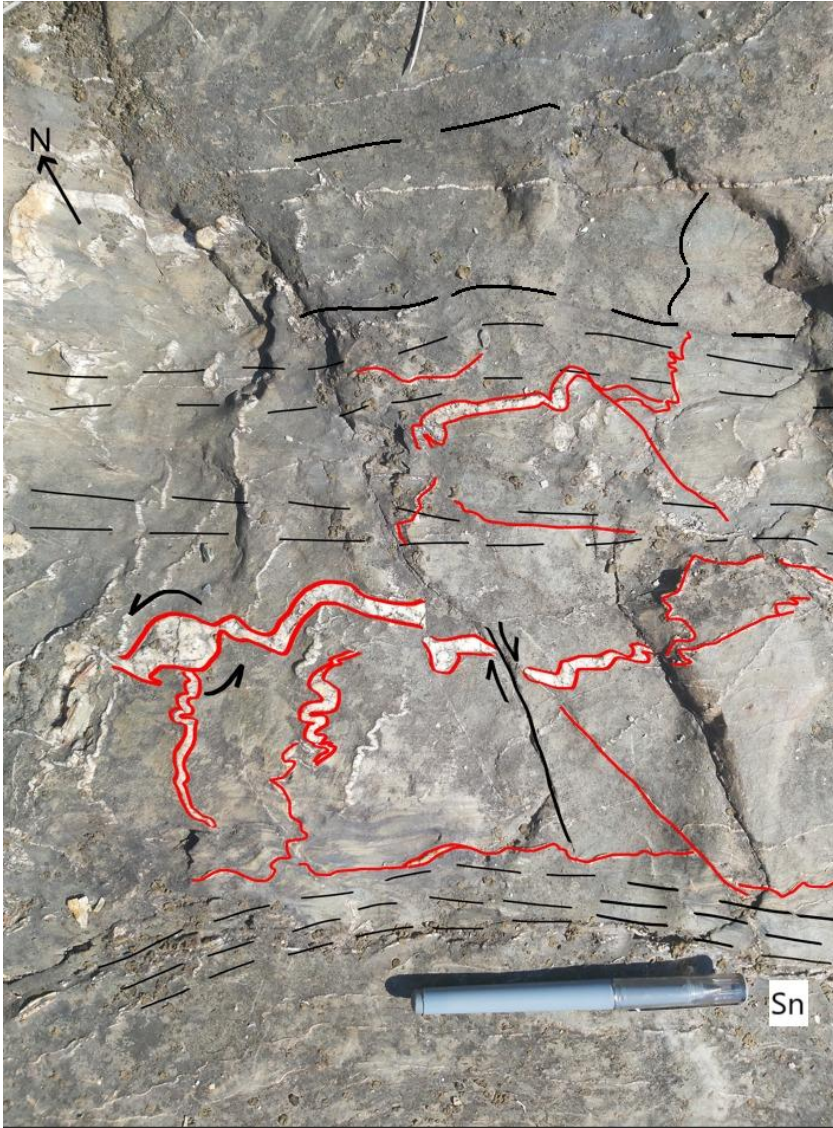
Figure 6.11 – Photo interpretation with the quartz veins in red, late brittle faults and kinematics in black. Dashed lines represent the transposed bedding planes ($S_0//S_n$).

Figure 6.12 – Photo interpretation of the quartz veins, a single observed fault and $S_0//S_n$.

6.2   Microtectonics

Six samples were carefully collected for the microtectonics study of the cross sections 1 and 2 (samples with prefix "PER") and of the riverbed exposures (prefix "RIO"). Sample PER-2.1 is an oriented sample with the foliation attitude of 50º/065º (dip/dip azimuth nomenclature). Sample PER-2.2 has no orientation, and it was collected to determine fabric relationships. Sample PER-6.1 is oriented and presents a main foliation of 54º/080º. Sample PER-10.1 presents a foliation orientation of 60º/140º. Sample RIO-E.1 is oriented and presents a foliation of 50º/105º. Finally, sample RIO-3.1 presents a foliation of 70º/155º (Fig. 6.13).
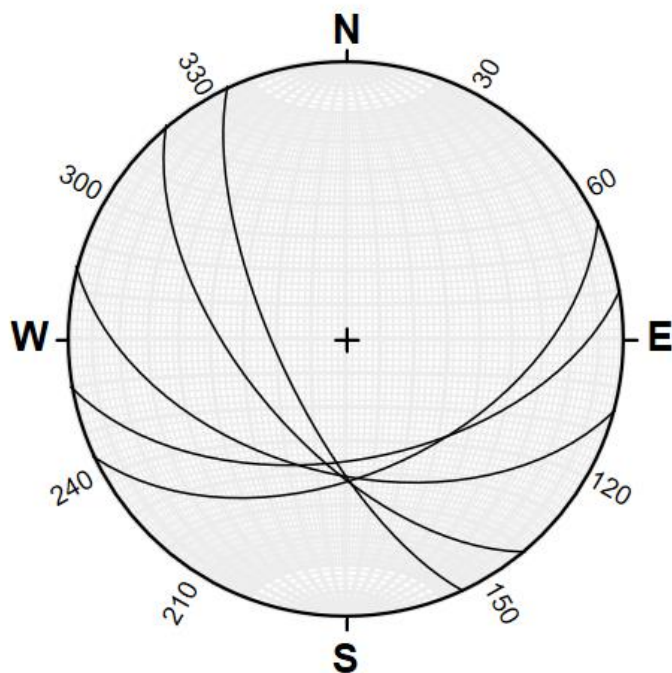
Figure 6.13 – Stereographic projection of the foliation of the oriented collected samples.

Oriented samples were cut in two orthogonal sections perpendicular to the main foliation (S_n), A and B, respectively one parallel to the stretching lineation (Fig. 6.14) and the other perpendicular to it (Fig. 6.15). Thin sections were made in all rock slices, including sample PER-2.2. All samples present a mineral association representing the chlorite-biotite zone of the greenschist facies metamorphism. General mineralogy is, in order of greatest abundance, composed of biotite, quartz, chlorite plagioclase and opaque minerals, including oxides and sulfides (pyrite).

In general, thin sections labeled as A show better evidence of the ductile tectonics associated to the deformation of the early quartz-veins, whereas sections B present evidence of related structures and later folding events. Also, in the B sections, some primary textures are also better preserved than in A.

There is a preferential orientation of the minerals defining a main foliation (S_n) that crenulate a previous foliation (S_{n-1}) and the bedding (S_0). The S_n compositional layering is formed by the preferential orientation of phyllosilicates (biotite->chlorite) and plastically deformed relict quartz grains.

6.2.1 Thin sections A

In oriented thin section PER-2.1A (Fig. 6.14A) the relationship between the C, C' shear bands and S_n is evident. The C shear planes show the main movement surface present in the thin sections, while the C'-shear bands represent the latter accommodation of that movement originating smaller shear zones with an angular relationship of 20 degrees with C. The $S_0//S_n$ is mostly given by the preferred orientation of the elongated quartz veins and the biotite, is inclined to SSE. $S_0//S_n$ is intersected and closely associated to the shear zones being cut and undulated giving indications of kinematics towards E to SSE.

Thin section PER-2.2A contains an intensely deformed quartz vein showing evidence of intracrystalline deformation with production of new polygonal grains with lattice preferred orientations. This originally planar vein is folded (isoclinal folds) with axial planes parallel to S_n and to the fold limbs, evidence of fabric transposition. Foliation is locally cutting the quartz vein

in the limbs, indicating refraction from the main foliation trend that wraps it, and shows the composite and dynamic nature of S_n with a primary $S_{n(a)}$ followed by intrafolial folding and transposition by $S_{n(b)}$ (Fig. 6.14B).

Thin section PER-10.1A (Fig. 6.14C) is oriented along the stretching lineation, and it also shows C-S shear bands. Quartz-rich layers appear separated by phyllosilicate bands mainly composed of biotite. Relict quartz grains are rounded to sub-rounded, with coarser grain sizes than in the other thin sections evidencing primary sedimentary aspects that are still preserved in these highly sheared rocks. The coarser aspect of quartz induced a more spaced aspect of the secondary C'-S shear bands that accommodated the deformation creating sigmoidal shapes of the pressure shadows around quartz grains that point for a top-to-SSE kinematics.

The oriented thin section PER-6.1A (Fig. 6.14D) shows complex shear zone fabrics, including C and C'-S shear bands and bookshelf boudinage affecting an early-S_n quartz-vein. The boudin-like structures are surrounded by a matrix made of fine-grained biotite and minor quartz grains. Boudinage was controlled by C'-S shear bands that accommodated a counterclockwise rotation of individual boudins, orthogonal to the quartz vein direction. The relationship of S_n with the two types of shear bands and boudinage is evident, and together they define a top-to-E kinematics along the stretching lineation identified in the cross section.

Oriented thin-section RIO-E.1A (Fig. 6.14E) is composed of biotite defining S_n that surrounds sigma-shaped relict quartz grains and is associated to C and C' shear bands. This deformation is sub-parallel to a highly recrystallized quartz vein, presenting signs of boudinage. Biotite and oxides are more concentrated along the main shear bands (C) while the C'-S present an anastomosed aspect, defining sigma shaped structures. Altogether, a consistent top-to-ESE kinematics can be inferred in this thin section.

In the oriented thin-section RIO-3.1A (Fig. 6.14F) sigma-shaped relict quartz grains and biotite define the matrix evidence of the presence of C- and C'-S structures with both top-to-NW and top-to-SE kinematics. This points out that pure shear may be present in the formation of this shear zones, confirming the role of deformation partitioning in this situation.
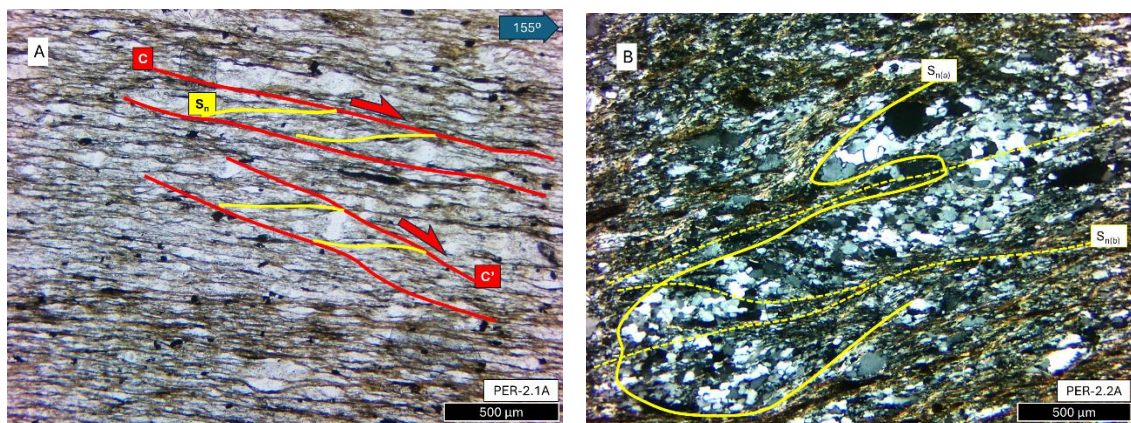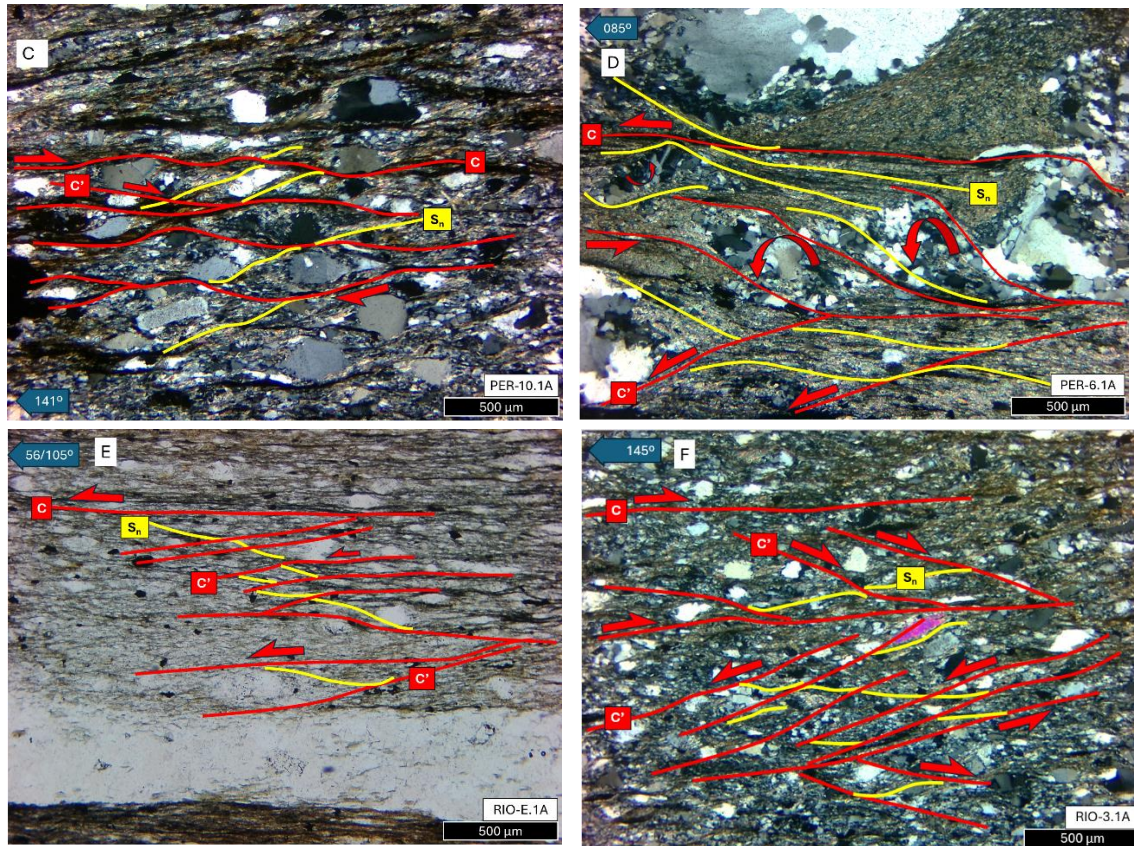
Figure 6.14 – Photomicrographs of the studied thin sections labeled as A (parallel to the stretching lineation/tectonic transport lineation). A) Simple shear criteria was observed by the presence of C-S and C'-S shear bands with top to SE shear movement (azimuth 155°) (parallel polarized light - PPL); B) Folded quartz-vein with composite S_n foliation with formation of intrafolial folds affecting an early $S_{n(a)}$, with axial planar $S_{n(b)}$ formed during the same tectono-metamorphic process (crossed polarized light - XPL); C) Simple shear defined by C-S bands, composing an apparent "augen" texture (XPL); D) Bookshelf boudinage on a quartz vein as result of C- and C'-S shear bands (XPL); E) Simple shear cutting through the Sn foliation being accommodated by C' (PPL); F) Conjugated C- and C'-S shear bands indicating pure shear (XPL). Matrix in all thin sections is composed of chlorite, biotite, muscovite, quartz, plagioclase and opaque minerals.

6.2.2 Thin sections B

The thin section PER-2.1B (Fig. 6.15A) represents a fine grained metapelite showing the main foliation (S_n) transposing the bedding, as highlighted by intercalations quartz rich and phyllitic layers that are parallel to the cleavage, The most micaceous layers present relicts of quartz grains with lenticular symmetrical shapes (orthorhombic symmetry). The main foliation is gently folded forming kink-like bands with axial planes parallel to S_{n+1}, which is not well developed in this sample.

Thin section PER-2.2B (Fig. 6.15B and C) is composed of a mostly phyllitic matrix with fine grained, gently recrystallized relict quartz and rare undeformed plagioclase grains. Micas define the main foliation parallel to the bedding ($S_0//S_n$), which is coetaneous with the formation of C and C' shear bands and parallel to sub parallel to mylonitized or intensely recrystallized quartz veins (Fig. 6.15B). Locally C-S shear bands also affect quartz veins that are also highly stretched producing necking zones of boudins. The surface of these necking zones represents simple shear zones. Between S_n cleavage domains, relicts of a previous foliation (S_{n-1}) are still preserved, defining M shaped crenulations marking intrafolial folds related to the simple shear and pure shear components of the shearing along C-S_n shear bands. This is evidence of a precursor folding stage not represented in the studied exposures. All the described fabrics were affected by a latter

35

folding stage, producing cylindrical microfolds with Sn+1 axial planar cleavage (Fig 6.15C)

Thin section PER-6.1B (Fig. 6.15D) reinforces the presence of an early foliation (S_{n-1}) defined by biotite and precursor quartz veins, preserved in the microlithons of the crenulation cleavage domains of S_n. In this situation, the main foliation is also defined by the accumulation of oxides along evidencing pressure-solution processes synchronous with the transposition of the early fabrics and with boudinage of sub-parallel quartz veins (these also presenting a salvage of misoriented biotite to chlorite blasts).

In thin section RIO-E.1B (Fig. 6.15E) two different domains are observed, separated by a transposing tectonic surface that is mimetic of the original bedding. The most pelitic domain shows biotite forming with a very pervasive S_n cleavage that is crenulated by microfolds with Sn+1 axial planar, rough and spaced cleavage, which is also affecting the coarser grained layer. The most quartzitic domain showing coarse-grained relict quartz and minor plagioclase, has lenticular recrystallized quartz in the matrix and a quartz vein affected by a folded C-S shear band that has no continuity to the pelitic layer, evidencing that the C-shear band at the boundary of both layers has helped to transpose the primary fabrics in this situation.

RIO-3.1B thin section (Fig. 6.15F) presents tight intrafolial, isoclinal folds with Sn as an axial plane cleavage. These folds seem to be affecting a previous boudinage pattern in the quartz vein, as response to the shearing in the perpendicular direction to this cross section. Also, it evidences the composite nature of S_n, with a precursor stage where foliation was parallel to the quartz vein being folded during latter stages. As in the previous cases, a S_{n+1} axial planar foliation is developed in response to the crenulation of the syn-S_n fabrics.
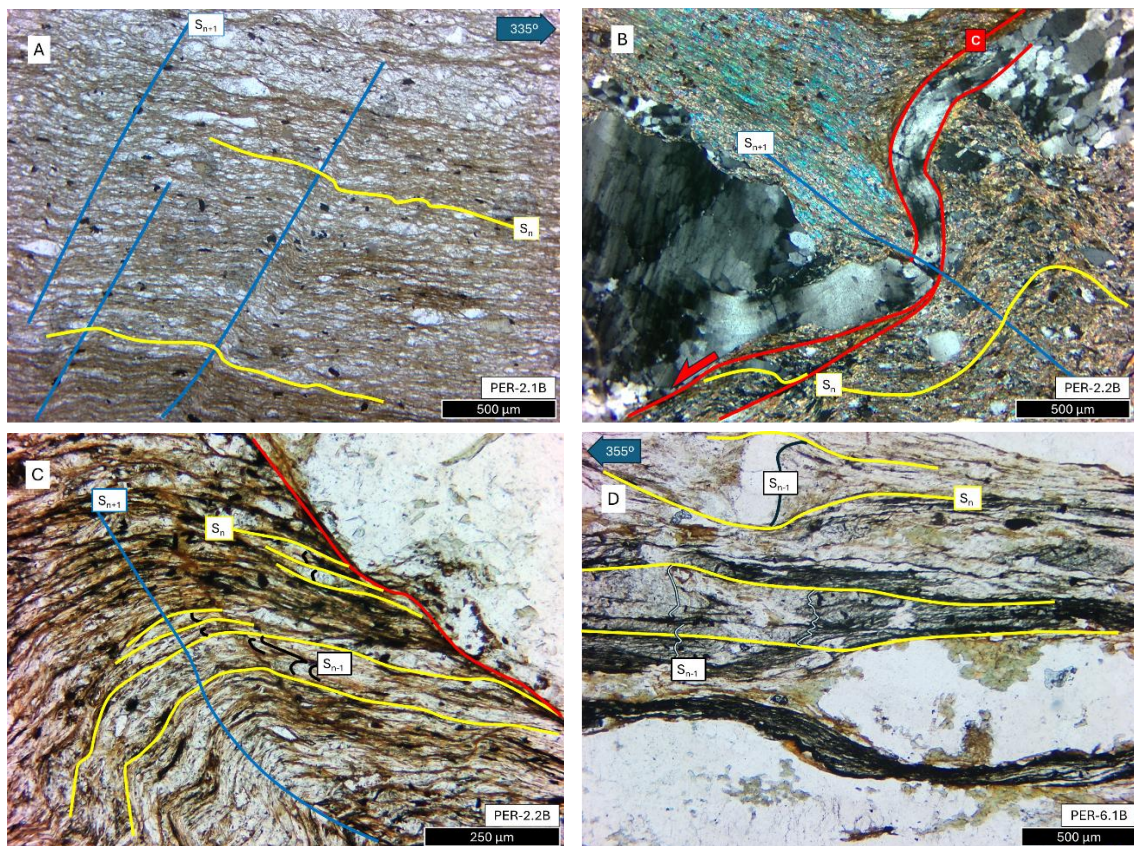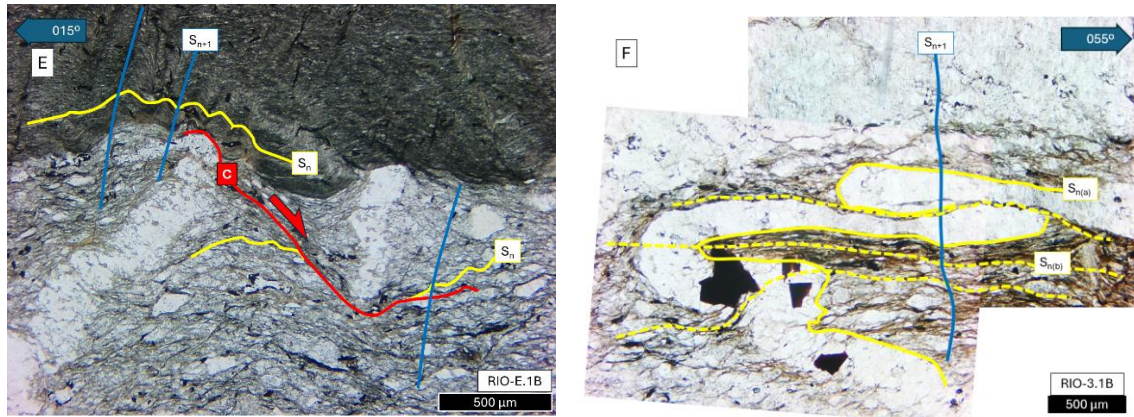
Figure 6.15 – Photomicrographs of the studied thin sections labeled as B (perpendicular to the stretching lineation/tectonic transport lineation). A) Late crenulation (S_{n+1}) affecting the main foliation that is transposing bedding (S_0//S_n) (PPL); B) Thin section with necking on quartz vein and the foliation accommodating the deformation showing the late crenulation (XPL); C) Late crenulation (S_{n+1}) related to cylindrical folding affecting S_0//S_n, with the preservation of earlier fabrics (S_{n-1}) (PPL); D) Early foliation (Sn-1) preserved in the microlithons of S_n (PPL); E) Quartz veins and their relationship with the S_0//S_n affected by late crenulation (PPL); F) Composite cleavage and isoclinal folds in syn-S_n quartz vein with transposition in the limbs (PPL). Matrix in all thin sections is composed of chlorite, biotite, muscovite, quartz, plagioclase and opaque minerals.

7. Discussion

7.1 Deformation sequence

The deformation observed in the outcrops in the study area began with a process of folding possibly in the chlorite zone of the greenschist facies. This precursory folding developed an axial planar S_{n-1} foliation, which should be in a close to upright position due to the orthogonal geometry in respect to S_n, and started with the transposition process, under low metamorphic conditions of the bedding in this sector of the Malpica do Tejo Fm. The tectonic reorganization of metapelite, metasiltite and metagraywacke beds was forced by the preservation of more quartzitic materials in the hinges of folds and by pressure solution processes along the limbs, as the quartz veins were being formed along and perpendicular to the foliation planes.

Increasing deformation in the biotite zone, associated to the emplacement of a ductile to semi-ductile shear zone, has increased flattening of the previous fabrics and allowed the total transposition of the bedding by a new composite foliation (S_n as $S_{n(a)}$ and $S_{n(b)}$) associated to intrafolial folds and a general top-to-E to SSE simple shear, which favored the increasing of the pressure solution of quartz in the matrix and the development of a large amount of millimetric to centimetric quartz veins, preserving a well-developed stretching lineation, forming geometries similar to the ones described in Fig. 5.5. This shear zone was complemented by a local top-to-WNW conjugate movement that evidences a pure shear component and the deformation partitioning revealing inhomogeneous deformation. Ductile shear implies a progressive sliding movement along the stretching lineation, which is currently tilted approximately 70º to the east (approximately), produced by a latter folding that acted in the chlorite zone and locally steepened the syn-S_n fabrics, as expressed by the microfolding and axial planar S_{n+1} foliation. At its origin, this lineation was closer to a sub-horizontal position, suggesting that the initial movement could have been mainly extensional. If this is the case, these shear zones were produced by a major detachment involving the Malpica do Tejo Fm. metasediments in this area.

Folding of S_n and associated fabrics and the crenulation of S_{n-1} foliation is more evident in the B thin sections, perpendicularly to the stretching lineation in the syn-kinematic quartz veins where curtain folds were developed. Also, in the studied exposures, namely in the Tejo riverbed outcrops which nearly correspond to the B sections, it is possible to observe the geometry of the brittle

faults associated folds, with a clear relationship of the main (S_n) foliation and the deformation associated to the later brittle deformation regime. The spatial distribution of these faults and folds also contributes to our understanding of the deformation patterns in the area and how tectonic forces have been distributed over time.

This late brittle deformation regime, generated N-S vertical faults and sub-horizontal joints and faults and produced centimetric to metric scale vertical and sub-horizontal axial plane kink-bands. These kink-bands occur near fault surfaces or in areas of more intense brittle shearing in shallow upper crust conditions. The presence of these structures shows that there has been a geometric reorganization of the previous structures, including foliations and stretching lineation, causing a local rotation of the tectonic fabrics both vertically and horizontally. This type of distortion intensifies the complexity of the deformed structures, making it difficult to interpret older movements and amplifying the depression of the ductile deformation elements in the outcrops we studied.

7.2   Correlation of fabrics with the regional deformation scheme

In terms of regional structural interpretation, the S_n local foliation could match the regional Variscan S_2 foliation, associated to the superstructure of the D_2-M_2 extensional event. In this situation, the preservation of a former foliation associated with the D_1-M_1 compressional stage is possible in the crenulation cleavage domains of S_2, as described elsewhere in the Iberian Massif, including the Central Iberian Zone (CIZ). In this situation, the local S_{n-1} cleavage could represent the S_1 axial plane foliation of upright folds formed in the chlorite zone in the CIZ. The relationship between these two foliations is crucial to understanding the process of deformation evolution, as the presence of S_2 indicates a new phase of deformation that has overlapped the previous foliation and formed new deformation structures but preserving traces of the older deformation. Both S_1 and S_2 foliations are regionally affected by a new stage of compressional deformation, the regional D_3-M_3, which led to upright disharmonic folding, and it is contemporaneous with regional uplift of the Variscan orogenic roots, which generates an S_3 axial plane cleavage that can correspond to the local S_{n+1}. These final stages of brittle deformation could be associated with the late-D_3 compression that produced northward brittle shear-zones, and a metric spaced jointing and folding, as described in nearby sectors of the CIZ.

In summary deformation in the studied sector can be directly associated with the three stages of the Variscan tectono-metamorphic cycles (Fig. 7.1): D_1 (with the C_1 folding and Barrovian event), D_2 (to the E_1 extensional event) and D_3 (C_3 folding and uplift). D_1 would correspond to the initial crustal thickening, associated with ductile folding processes and the formation of the S_1 foliation. D_2, in turn, reflects the deformation associated with the sub-horizontal crenulation of S_1 by S_2, with the increase in deformation intensity near shear bands, and marking the thermal/metamorphic peak (M_2). D_3 is related to the folding and formation of an upright S_3 axial plane cleavage related to the final orogenic uplift and regional metamorphic retrogression.

In the absence of more direct chronological evidence, such as absolute dating or specific stratigraphic evidence, it is reasonable to infer that the deformations observed are related to the Variscan tectonic cycle, since Cadomian deformation, which could be an alternative, has not yet been confirmed for this sector of the Central Iberian Zone. This implies that the tectonic events in the area are more likely Variscan, in line with what is described for this sector of the Iberian Massif.
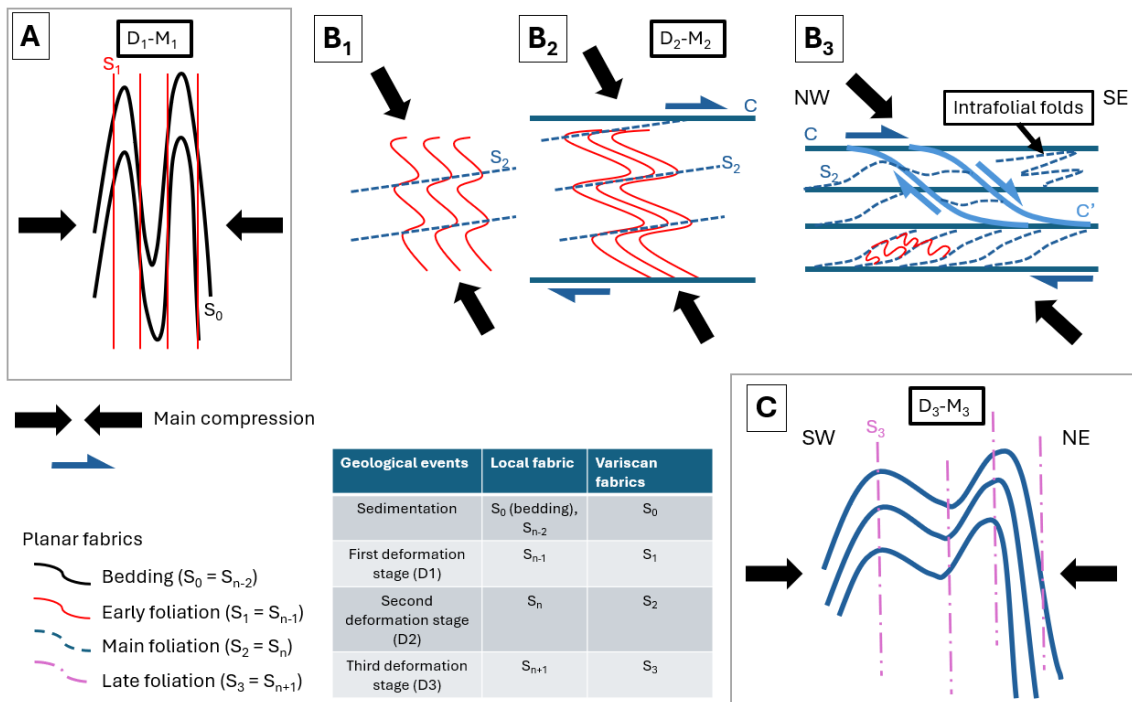
Figure 7.1 – Scheme representing the deformation that occurred in the studied exposures and thin sections and table with the correlation of local with regional Variscan fabrics. Image A represents the deformation that occurred during the first compressional stage, with folding of bedding with vertical axial planes. Image B shows the transposing of the foliation from the previous deformation event during simple shear with top-to-ESE or to SSE. C) simplifies the latest deformation event responsible by the folding of the previous foliations.

8. Conclusions

The macro to microscale study of the complex structural elements of the Perais picnic area has revealed an intricate deformation process probably associated with the Variscan orogenic cycle, affecting the detrital rocks of the Ediacaran Schist and Graywacke Complex of the Central Iberian Zone. The deformation patterns include complex folding of quartz veins and the complete transposition of the original bedding, leading to a sequence of overprinting fabrics only observable under petrographic microscope, and using the standard techniques of microtectonics to study and to identify the different fabrics. This process helped to successfully identify different heterogeneous deformation events in low metamorphic grade conditions that, in a first stage, has produced folding and formation of an axial planar foliation (S_{n-1}) in the chlorite zone, progressing through increasing deformation in the biotite zone, where a ductile, simple shear has dominated. This led to the transposition of bedding by the main foliation (S_n) and the development of complexly folded quartz veins and a stretching lineation along which a general top-to-ESE and local top-to-WNW shear movements, mark a phase of partitioned deformation. The late stages of ductile deformation has produces upright folding with axial planar foliation (S_{n+1}), a regime that gradually progressed into a brittle deformation that influenced the appearance of vertical faults, sub-horizontal jointing and associated kink-bands, favoring the reorganization of the previous structures. The regional tectonic framework indicates that these deformation stages align with the Variscan tectono-metamorphic cycle, specifically with D_1 (crustal thickening and folding), D_2 (extensional events and metamorphic peak), and D_3 (folding, uplift, and retrogression), as there is no evidence to support the involvement of Cadomian deformation in this part of the Central Iberian Zone.

Bibliography

Amaral, F., Dias, R., Coke, C., Romão, J., & Ribeiro, A. (2014). A fase de deformação sarda na Zona Centro-Ibérica The Sardic deformation in Central-Iberian Zone.

Arenas R, Abati J, Catalán JRM, García FD, Pascual FJR (1997) P-T evolution of eclogites from the Agualada Unit (Ordenes Complex, northwest Iberian Massif, Spain): Implications for crustal subduction. Lithos 40 (2):221-242. doi:10.1016/S0024-4937(97)00029-7

Arenas R, Novo-Fernández I, Garcia-Casco A, Díez Fernández R, Fuenlabrada JM, Pereira MF, Abati J, Sánchez Martínez S, Rubio Pascual FJ (2021) A unique blueschist facies metapelite with Mg-rich chloritoid from the Badajoz-Córdoba Unit (SW Iberian Massif): correlation of Late Devonian high-pressure belts along the Variscan Orogen. International Geology Review 63 (13):1634-1657. doi:10.1080/00206814.2020.1789509

Chichorro M, Solá AMR, Bento dos Santos T, Amaral JL, Crispim L (2023) Cadomian/Pan-African consolidation of the Iberian Massif assessed by its detrital and inherited zircon populations: is the~ 610Ma age peak a persistent Cadomian magmatic inheritance or the key to unravel its Pan-African basement? Geologica Acta 20 (2):1-29. doi:10.1344/GeologicaActa2022.20.15

Dallmeyer RD, Martínez Catalán JR, Arenas R, Gil Ibarguchi JI, Gutiérrez-Alonso G, Farias P, Bastida F, Aller J (1997) Diachronous Variscan tectonothermal activity in th NW Iberia Massif: Evidence from 40Ar/39Ar dating of regional fabrics. Tectonophysics 277 (4):307-337. doi:10.1016/S0040-1951(97)00035-8

Dallmeyer, R. D., & Garcia, E. M. (Eds.). (1990). Pre-Mesozoic Geology of Iberia. Springer Berlin Heidelberg. https://doi.org/10.1007/978-3-642-83980-1

Dias da Silva, Í. (2013). Geología de las zonas Centro Ibérica y Galicia – Trás-Os-Montes en la parte oriental del Complejo de Morais, Portugal/España [Universidad de Salamanca]. https://doi.org/10.14201/gredos.121357

Dias da Silva, Í., González Clavijo, E., & Díez-Montes, A. (2021). The collapse of the Variscan belt: A Variscan lateral extrusion thin-skinned structure in NW Iberia. International Geology Review, 63(6), 659–695. https://doi.org/10.1080/00206814.2020.1719544

Dias da Silva, Í., Martins, I., Mateus, A., (2023). Does the lithostratigraphic harmonization of the Beiras Group (Panasqueira-Segura area) disclose any pre-Ordovician structure? Livro de Resumos do XI Congresso Nacional de Geologia, Universidade de Coimbra, Coimbra, 187-188.

Dias R, Ribeiro A (2013) O Varisco do sector norte de Portugal. In: Dias R, Araújo A, Terrinha P, Kullberg JC (eds) Geologia de Portugal, vol Vol. I - Geologia Pré-mesozoica de Portugal. Escolar Editora, Lisboa, pp 59-71

Díez Balda MA, Vegas R, González Lodeiro F (1990) Structure. In: Dallmeyer RD, Martínez García E (eds) Pre-Mesozoic Geology of Iberia. Springer-Verlag, Germany, pp 172-188

Díez Fernández R, Arenas R, Pereira MF, Martínez SS, Albert R, Parra LMM, Pascual FJR, Matas J (2016) Tectonic evolution of Variscan Iberia: Gondwana–Laurussia collision revisited. Earth-Science Reviews. doi:10.1016/j.earscirev.2016.08.002

Díez Fernández R, Pereira MF (2017) Strike-slip shear zones of the Iberian Massif: Are they coeval? Lithosphere 9 (5):726-744. doi:10.1130/L648.1

Ellouz N, Patriat M, Gaulier JM, Bouatmani R, Sabounji S (2003) From rifting to Alpine inversion: Mesozoic and Cenozoic subsidence history of some Moroccan basins: Sed Geol 156: 185–212, https:// doi.org/10.1016/s0037-0738(02)00288-9

Escuder Viruete J, Arenas R, Martínez Catalán JR (1994) Tectonothermal evolution associated with Variscan crustal extension, in the Tormes Gneiss dome (NW Salamanca, Iberian Massif, Spain). Tectonophysics 238:1-22. doi:10.1016/0040-1951(94)90052-3

Escuder Viruete J, Hernáiz Huerta PP, Valverde-Vaquero P, Rodríguez Fernández R, Dunning GR (1998) Variscan syncollisional extension in the Iberian Massif: structural, metamorphic and geochronological evidence from the Somosierra sector of the Sierra de Guadarrama (Central Iberian Zone, Spain). Tectonophysics 290 (1-2):87-109. doi: 10.1016/S0040-1951(98)00014-6

Ferreira da Silva, A. (2013). A Litostratigrafia e Estrutura do Supergrupo Dúrico-Beirão (Complexo Xisto-Grauváquico), em Portugal, e sua correlação com as correspondentes sucessões em Espanha. Boletim de Minas 48, (2), 97-142.

Fossen, H. (n.d.). Structural Geology.Geological structures and maps: A practical guide (3rd ed). (2007). Elsevier Butterworth Heinemann.

Fuenlabrada JM, Arenas R, Sánchez Martínez S, Díez Fernández R, Pieren AP, Pereira MF, Chichorro M, Silva JB (2020) Geochemical and isotopic (SmNd) provenance of Ediacaran-Cambrian metasedimentary series from the Iberian Massif. Paleoreconstruction of the North Gondwana margin. Earth-Science Reviews 201:103079. doi:10.1016/j.earscirev.2019.103079

Gutiérrez-Alonso G, Collins AS, Fernández-Suárez J, Pastor-Galán D, González-Clavijo E, Jourdan F, Weil AB, Johnston ST (2015) Dating of lithospheric buckling: 40Ar/39Ar ages of syn-orocline strike–slip shear zones in northwestern Iberia. Tectonophysics 643:44-54. doi:10.1016/j.tecto.2014.12.009

Gutiérrez-Marco JC, Piçarra JM, Meireles CA, Cózar P, García-Bellido DC, Pereira Z, Vaz N, Pereira S, Lopes G, Oliveira JT, Quesada C, Zamora S, Esteve J, Colmenar J, Bernárdez E, Coronado I, Lorenzo S, Sá AA, Dias da Silva Í, González-Clavijo E, Díez-Montes A, Gómez-Barreiro J (2019) Early Ordovician–Devonian Passive Margin Stage in the Gondwanan Units of the Iberian Massif. In: Quesada C, Oliveira JT (eds) The Geology of Iberia: A Geodynamic Approach: Volume 2: The Variscan Cycle. Springer International Publishing, Cham, pp 75-98. doi:10.1007/978-3-030-10519-8_3

Julivert M, Fonboté JM, Ribeiro A, Conde L (1972) Memoria explicativa del Mapa Tectónico de la Península Ibérica y Baleares. Escala 1:1.000.000. Instituto Geológico y Minero de España, Madrid

López-Moro FJ, López-Plaza M, Gutiérrez-Alonso G, Fernández-Suárez J, López-Carmona A, Hofmann M, Romer RL (2018) Crustal melting and recycling: geochronology and sources of Variscan syn-kinematic anatectic granitoids of the Tormes Dome (Central Iberian Zone). A U-Pb LA-ICP-MS study. International Journal of Earth Sciences 107 (3):985-1004. doi:10.1007/s00531-017-1483-8

Martínez Catalán JR (2012) The Central Iberian arc, an orocline centered in the Iberian Massif and some implications for the Variscan belt. International Journal of Earth Sciences 101 (5):1299-1314. doi:10.1007/s00531-011-0715-6

Martínez Catalán JR, Arenas R, Abati J, Sánchez Martínez S, Díaz García F, Fernández-Suárez J, González Cuadra P, Castiñeiras P, Gómez Barreiro J, Díez Montes A, González Clavijo E, Rubio Pascual F, Andonaegui P, Jeffries TE, Alcock JE, Díez Fernández R, López Carmona A (2009) A rootless suture and the loss of the roots of a mountain chain: The Variscan Belt of NW Iberia. CR Geoscience 341 (2-3):114-126. doi:10.1016/j.crte.2008.11.004

Martínez Catalán JR, Arenas R, Díaz García F, González Cuadra P, Gómez Barreiro J, Abati J, Castiñeiras P, Fernández-Suárez J, Sánchez Martínez S, Andonaegui P, González Clavijo E, Díez Montes A, Rubio Pascual F, Valle Aguado B (2007) Space and time in the tectonic evolution of the northwestern Iberian Massif: Implications for the Variscan belt. In: Hatcher Jr. RD, Carlson MP, McBride JH, Martínez Catalán JR (eds) 4-D Framework of Continental Crust, vol 200. Geologic Society of America, Boulder, pp 403-423. doi:10.1130/2007.1200(21)

Martínez Catalán JR, Rubio Pascual F, Díez Montes A, Díez Fernández R, Gómez Barreiro J, Dias da Silva Í, González Clavijo E, Ayarza Arribas P, Alcock JE (2014) The late Variscan HT/LP

metamorphic event in NW and central Iberia: Relationships with crustal thickening, extension, orocline development, and crustal evolution. In: Schulmann K, Martínez Catalán JR, Lardeaux JM, Janousek V, Oggiano G (eds) The Variscan Orogeny: Extent, Timescale and the Formation of the European Crust, vol 405. Geological Society, London, Special Publications, London, pp 225-247. doi:10.1144/SP405.1

Martínez Catalán, J.R. (2011). Are the oroclines of the Variscan belt related to late Variscan strike-slip tectonics? Terra Nova, 23, 241-247, https://doi.org/10.1111/j.1365-3121.2011.01005.x.

Meireles, C. (coord.) (2020). Folha 4 da Carta Geológica de Portugal, na escala 1:200 000. LNEG, Lisboa.

Meireles, C., Castro, P., & Ferreira, N. (2014). Evidências cartográficas, litoestratigráficas e estruturais sobre a presença de discordância cadomiana intra Grupo das Beiras.

Metodiev, D., Romão, J., Dias, R., & Ribeiro, A. (n.d.). Sinclinal de Vila Velha de Ródão (Zona Centro-Ibérica, Portugal): Litostratigrafia, estrutura e modelo de evolução da tectónica Varisca.

Moita P, Munhá J, Fonseca PE, Pedro J, Tassinari CCG, Araújo A, Palácios T Phase equilibria and geochronology of Ossa-Morena eclogites. In: XIV Semana de Geoquímica - VIII Congresso de Geoquímica dos Países de Língua Portuguesa, Aveiro, 2005. Universidade de Aveiro, pp 463-466

Orejana D, Merino Martínez E, Villaseca C, Andersen T (2015) Ediacaran–Cambrian paleogeography and geodynamic setting of the Central Iberian Zone: Constraints from coupled U–Pb–Hf isotopes of detrital zircons. Precambrian Research 261:234-251. doi:https://doi.org/10.1016/j.precamres.2015.02.009

Passchier W.Cees, Trouw A.J. Rudolph. Microtectonics. Germany,Heilderbeg: Springer Berlin Heidelberg,2005

Pastor-Galán D, Dias da Silva Í, Groenewegen T, Krijgsman W (2019) Tangled up in folds: tectonic significance of superimposed folding at the core of the Central Iberian curve (West Iberia). International Geology Review 61 (2):240-255. doi:10.1080/00206814.2017.1422443

Pereira MF, Chichorro M, Williams IS, Silva JB, Fernández C, Díaz-azpíroz M, Apraiz A, Castro A (2009) Variscan intra-orogenic extensional tectonics in the Ossa-Morena Zone (Évora-Aracena-Lora del Río metamorphic belt, SW Iberian Massif): SHRIMP zircon U-Th-Pb geochronology. Geological Society, London, Special Publications 327 (1):215-237. doi:10.1144/sp327.11

Pereira MF, Linnemann U, Hofmann M, Chichorro M, Solá AR, Medina J, Silva JB (2012) The provenance of Late Ediacaran and Early Ordovician siliciclastic rocks in the Southwest Central Iberian Zone: Constraints from detrital zircon data on northern Gondwana margin evolution during the late Neoproterozoic. Precambrian Research 192-195:166-189. doi:10.1016/j.precamres.2011.10.019

Quesada, C., & Oliveira, J. T. (Eds.). (2019). The Geology of Iberia: A Geodynamic Approach: Volume 2: The Variscan Cycle. Springer International Publishing. https://doi.org/10.1007/978-3-030-10519-8

Quesada, C., & Oliveira, J. T. (Eds.). (2019). The Geology of Iberia: A Geodynamic Approach: Volume 3: The Alpine Cycle. Springer International Publishing. https://doi.org/10.1007/978-3-030-11295-0

Ribeiro, O., Teixeira, C., Carvalho, H., Peres, A. M., Fernandes, A. P. (1964). Carta Geológica de Portugal na escala 1:50.000, Folha 28-B (Nisa). Serviços Geológicos de Portugal, Lisboa.

Rodríguez Alonso MD, Peinado M, López-Plaza M, Franco P, Carnicero A, Gonzalo JC (2004) Neoproterozoic-Cambrian synsedimentary magmatism in the Central Iberian Zone (Spain): geology, petrology and geodynamic significance. International Journal of Earth Sciences 93

(5):897-920. doi:doi: 10.1007/s00531-004-0425-4

Romão, J. M., Coke, C., Dias, R., & Ribeiro, A. (2005). Transient inversion during the opening stageof the Wilson cycle "Sardic phase" in the Iberian Variscides –Stratigraphic and tectonic record. Geodinamica Acta, 18(2), 115–129. https://doi.org/10.3166/ga.18.115-129

Romão, J., & Ribeiro, A. (n.d.). Thrust tectonics of sardic age in the Rosmaninhal area (Beira Baixa, Central Portugal).

Sequeira, A. J. D. (2011). Microfósseis do Grupo das Beiras (Monfortinho – Salvaterra do Extremo, Beira Baixa, Portugal Central).

Smith, W. D., & Maier, W. D. (2021). The geotectonic setting, age and mineral deposit inventory of global layered intrusions. Earth-Science Reviews, 220, 103736. https://doi.org/10.1016/j.earscirev.2021.103736

Talavera C, Martínez Poyatos D, González Lodeiro F (2015) SHRIMP U–Pb geochronological constraints on the timing of the intra-Alcudian (Cadomian) angular unconformity in the Central Iberian Zone (Iberian Massif, Spain). International Journal of Earth Sciences 104 (7):1739-1757. doi:10.1007/s00531-015-1171-5

Valladares MI, Barba P, Ugidos JM, Colmenero JR, Armenteros I (2000) Upper Neoproterozoic–Lower Cambrian sedimentary successions in the Central Iberian Zone (Spain): sequence stratigraphy, petrology and chemostratigraphy. Implications for other European zones. International Journal of Earth Sciences 89 (1):2-20. doi:doi: 10.1007/s005310050314

Vauchez, A. (1980). Ribbon texture and deformation mechanisms of quartz in a mylonitized granite of great kabylia (Algeria). Tectonophysics, 67(1–2), 1–12. https://doi.org/10.1016/0040-1951(80)90160-2

Weil AB, Gutiérrez-Alonso G, Conan J (2010) New time constraints on lithospheric-scale oroclinal bending of the Ibero-Armorican Arc: a palaeomagnetic study of earliest Permian rocks from Iberia. Journal of the Geological Society 167:127-145. doi:10.1144/0016-76492009-002